

**ART End User Applications
Task 2.04.19.06
Supercritical Transformational Electric Power (STEP)**

Milestone Report

Foil Bearing Coating Behavior in CO₂

Matthew Walker ^[A], Alan Kruizenga ^[A], James Pasch ^[B], and Darryn Fleming ^[B]

*Sandia National Laboratories
Livermore, CA ^[A]
Albuquerque, NM ^[B]*

August 1, 2017

S-CO₂ Materials Development
Work Package: AT-17SN190602 (STEP – 2)
Level 3 Milestone Report: M3AT-17SN1906025

ABSTRACT

The Sandia S-CO₂ Recompression Closed Brayton Cycle (RCBC) utilizes a series of gas foil bearings in its turbine-alternator-compressors. At high shaft rotational speed these bearings allow the shaft to ride on a cushion of air. Conversely, during startup and shutdown, the shaft rides along the foil bearing surface. Low-friction coatings are used on bearing surfaces in order to facilitate rotation during these periods. An experimental program was initiated to elucidate the behavior of coated bearing foils in the harsh environments of this system. A test configuration was developed enabling long duration exposure tests, followed by a range of analyses relevant to their performance in a bearing. This report provides a detailed overview of this work. The results contained herein provide valuable information in selecting appropriate coatings for more advanced future bearing-rig tests at the newly established test facility in Sandia-NM.

CONTENTS

1. <u>Introduction</u>	5
2. <u>Background</u>	5
2.1. Bearings Overview.....	5
2.2. Gas Foil Bearings.....	6
2.3. Bearings for S-CO ₂ Power Systems.....	8
2.4. Sandia RCBC System	9
2.5. Identified Research Needs for S-CO ₂ System Gas Foil Bearings.....	12
3. <u>Approach</u>	12
3.1. Identification of Candidate Foil Coating Materials.....	13
3.1.1. Xdot Engineering and Analysis	13
3.1.2. Mechanical Solutions	15
3.2. Exposure Furnace Setup	16
3.3. Test Sample Characterization.....	19
3.3.1. Visual.....	20
3.3.2. Weight Change.....	20
3.3.3. Coating/Substrate Microstructure.....	20
3.3.4. Surface Roughness.....	21
3.3.5. Scratch Testing.....	22
4. <u>Results</u>	24
4.1. Visual.....	24
4.2. Weight Change.....	27
4.3. Coating/Substrate Microstructure.....	28
4.4. Surface Roughness.....	33
4.5. Scratch Testing.....	36
5. <u>Summary</u>	38
6. <u>References</u>	39

FIGURES

Figure 1. Two Main Categories of Continuous Rotation Bearings.....	6
Figure 2. Three types of gas foil radial bearings.....	7
Figure 3. Typical construction for bump foil journal and thrust bearings.....	8
Figure 4. Types of bearings proposed for use in S-CO ₂ applications.....	9
Figure 5. Diagram of Sandia's S-CO ₂ TAC showing the location for the bearings.....	11
Figure 6. Images of the gas foil radial bearings used in Sandia's S-CO ₂ RCBC loop	11
Figure 7. Images of the gas foil axial bearing used in Sandia's S-CO ₂ RCBC loop.....	11
Figure 8. Sample formats used for gas foil bearing performance evaluations.....	14
Figure 9. SEM images of a sample with the TX1 nitride surface treatment.....	14
Figure 10. EDS chemical analysis for the PS400 coating	15
Figure 11. Modified autoclave furnace for gas foil bearing tests at 300psi CO ₂	16
Figure 12. Sample holder configuration used for curved and flat foil samples.....	17
Figure 12. Sample holder loaded up with the full complement of samples.....	18
Figure 14. Sample types included in the higher temperature (550°C) exposure test.....	18
Figure 15. Sample types included in the lower temperature (315°C) exposure test	19
Figure 16. Surface roughness data provided for each measurement area for each sample....	21
Figure 17. Illustration of multiple elements to instrumented scratch testing	23
Figure 18. Samples on the holder following the two exposure experiments	24
Figure 19. Visual changes for flat foil samples before and after the 315°C exposure	25
Figure 20. Visual changes for non-flat foil samples before and after the 315°C exposure	26
Figure 21. Visual changes for flat foil samples before and after the 550°C exposure	26
Figure 22. Visual changes for non-flat foil samples before and after the 550°C exposure	27
Figure 23. Sample weight changes following the exposure tests at 315°C and 550°C.....	28
Figure 24. SEM cross-sections for one set of samples compared for the three conditions.....	30
Figure 25. SEM cross-sections for a 2 nd set of samples compared for the three conditions....	31
Figure 26. EDS chemical analysis for the TX1 coating exposed at 315°C.....	32
Figure 27. EDS chemical analysis for the TX1 coating exposed at 550°C.....	32
Figure 28. EDS chemical analysis for the 10K2 coating exposed at 550°C.....	33
Figure 29. EDS chemical analysis for the PS400 coating exposed at 550°C.....	33
Figure 30. Surface roughness measurements for the 315°C exposure test samples.....	34
Figure 31. 2D and 3D representations for surface roughness for the TX1 and WS ₂ samples..	35
Figure 32. Surface roughness measurements for the 550°C exposure test samples.....	35
Figure 33. Measured cohesive failure values for each coating material	37
Figure 34. Measured adhesive failure values for each coating material	37

TABLES

Table 1. Summary of Different Types of Bearings	6
Table 2. Descriptions of Bearing Foil Coating Materials	18
Table 3. Test Conditions and Parameters used for Instrumented Scratch Testing.....	23

1. Introduction

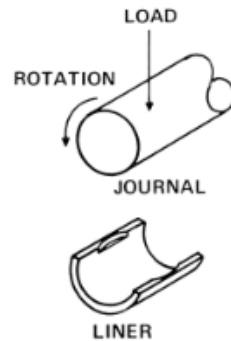
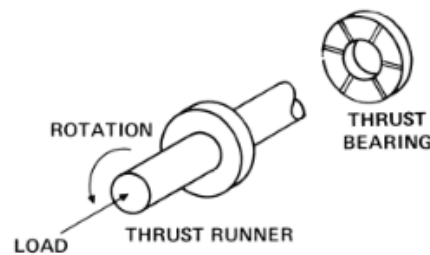
The supercritical carbon dioxide (S-CO₂) Brayton Cycle has gained significant attention in the last decade as an advanced power cycle capable of achieving high efficiency power conversion; it represents a thermal to electric energy conversion system with an efficiency approaching 50% under the operating conditions required for advanced energy systems. Sandia National Laboratories, with support from the U.S. Department of Energy Office of Nuclear Energy (US DOE-NE), has been conducting research and development in order to deliver a Recompression Closed Brayton Cycle (RCBC) that is ready for commercialization. There are a wide range of materials related challenges that must be overcome for the success of this technology. At Sandia, an area of recent focus has been on identifying the behavior of the coating materials used on gas foil bearings in the CO₂ environments relevant to these systems. At high shaft rotational speed these bearings allow the shaft to ride on a cushion of air. Conversely, during startup and shutdown, the shaft rides along the foil bearing surface. Low-friction coatings are used on bearing surfaces in order to facilitate rotation during these periods.

Through discussions with several of the companies that design and manufacture these types of bearings (Xdot Engineering and Analysis, Mechanical Solutions, and Mohawk Innovative Technology) it was realized that very little is known about the chemical compatibility of these coating materials with CO₂. Moreover, nothing is known about their behavior in CO₂ at conditions (pressure and temperatures) relevant to their application in an actual S-CO₂ bearing. It is of critical importance to understand the coating chemical behavior independent of mechanical loads. An experimental program was initiated to elucidate the behavior of coated bearing foils in the harsh environments of this system. A test configuration was developed enabling long duration exposure tests, followed by a range of analyses relevant to their performance in a bearing. This report provides a detailed overview of this work. The results contained herein provide valuable information in selecting appropriate coatings for more advanced future bearing-rig tests at the newly established test facility in Sandia-NM.

2. Background

2.1. Bearings Overview

In a general sense, a bearing is an element or assembly that guides or positions components subject to relative motion. For turbomachinery bearings, continuous rotation is required, and bearings are often classified as radial (journal) or axial (thrust) bearings. These are illustrated graphically in Figure 1, where the name of each derives from the positioning requirement. The fundamental requirement of a bearing is that it maintains the desired relative position, despite the forces or loads that must be transmitted. As such, it is important to minimize the wear which may be created by these surfaces under relative motion and load, and desirable to reduce the parasitic energy losses which invariably accompany bearings.

Radial Bearing**Axial (Thrust) Bearing****Figure 1. Two Main Categories of Continuous Rotation Bearings ^[1]**

Bearings can be categorized into four basic groups: rolling element, sliding element, magnetic, and fluid film. These four different groups of bearings are compared across a range of categories in Table 1. Selecting the appropriate bearing for an application will depend on cost, duty cycle, load, speed, size/weight, efficiency, and dynamic performance; the process can be rather complex as there are many factors to consider. The most common types of bearing used in land-based industrial turbomachinery are the fluid film bearings. The major advantage for fluid film bearings is their long life, resulting from non-wear operation. Also, in the case of the oil-lubricated fluid film bearings, the fluid film generates higher levels of damping than either rolling element bearing or magnetic bearing counterparts. Finally, fluid films can carry higher loads for longer periods than other bearings, making them prime candidates for heavily loaded land-based turbomachinery.

Table 1. Summary of Different Types of Bearings ^[2]

	Rolling element	Sliding element	Fluid film	Magnetic
Working medium	Gas/oil	Working fluid	Gas/oil	Working fluid
Shaft support	Rolling contact/ hydrodynamic lift	Sliding contact	Hydrodynamic/ Hydrostatic lift	Electromagnetic fields
Stiffness	High	Low	High	Medium
Damping	Low	Low	High	High
Load capacity	Medium	Low	High	Medium
Control	Passive	Passive	Passive	Active
Contacting	At low speed and excursions	Always	At low speed	Never
Cost	Low	Low	Medium	High
Drag torque	Low	Medium	Low-medium	Very low

2.2. Gas Foil Bearings

Gas foil bearings are a type of hydrodynamic fluid film bearing that has received significant interest in the development of R&D S-CO₂ power systems. While other types of bearings are also being used in S-CO₂ power systems, a more detailed overview of gas foil bearings is provided here as these have been the focus of recent research work at Sandia and directly relate to the work presented in this report.

Key attributes to gas foil bearings are that they are oil-free, compact, lightweight, and tolerant of high frequency-low displacement loads. Various designs for radial and thrust gas foil bearings exist. These include bump type, leaf type, and tape type. Schematics for these three types of gas foil bearings are shown in Figure 2. In each case the spinning shaft is supported on a thin film of air or process gas. No oil sealing or liquid lubrication is required. Due to there being no spinning parts to the bearing, they are well suited to high shaft speeds. With the elimination of lubrication, they are good for both low and high temperature operation. Furthermore, due to their flexible structure, they can tolerate significant shock loads, as well as substantial misalignment and dust/debris.

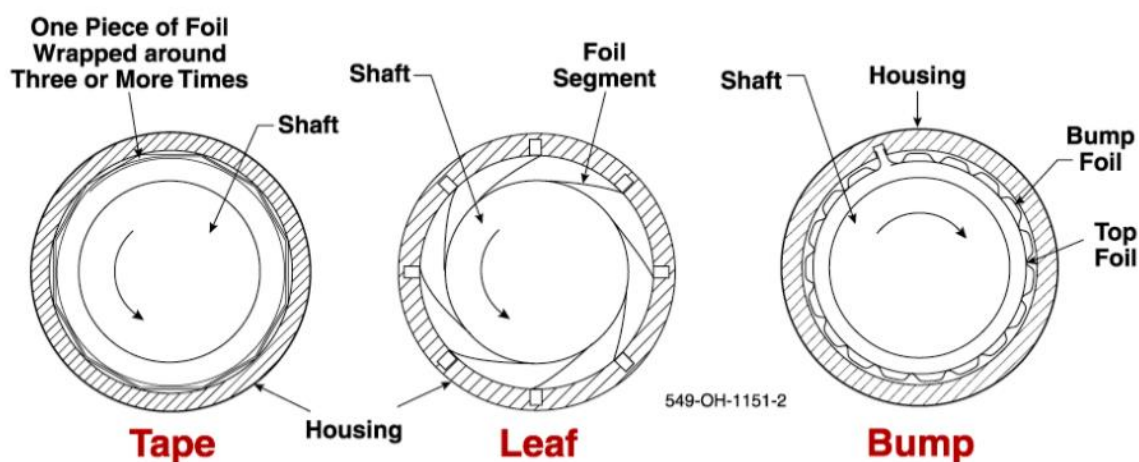


Figure 2. Three types of gas foil radial bearings ^[3]

Among the three type of gas foil bearings shown in Figure 2, the bump type has been the most popular. It is comprised of three basic components: a smooth top foil, a corrugated bottom foil or “bump foil”, and the support structure, usually a cylindrical shell for journal bearings and a flat disc for thrust bearings. Illustrations for these bump type foils are shown in Figure 3. Both the top and bottom foils are made from thin sheets of compliant metal, typically a nickel-based alloy such as Inconel X750. In a typical configuration, the top foil is affixed to the bearing housing at a point, and is initially allowed to sit to the height of its bump understructure. During loading and running, the foils are perturbed by the film pressure profile and resultant deflection of the foil bearing.

For normal, steady-state operation of these bearings, the shaft is supported on a fluid film, eliminating contact between the shaft and bearing. Conversely, at lower speeds during startup and shutdown, the shaft rides along the foil itself. To extend the life of the bearings and also to

facilitate rotation during these periods, coatings are applied to the top foil, the shaft journal, or both to minimize friction and wear. Important requirements for these surface coatings include chemical compatibility with the fluid environment, surface properties (surface roughness, coefficient of friction, etc.) to minimize abrasive wear and particle debris generation, and good adhesion to the metal substrate.

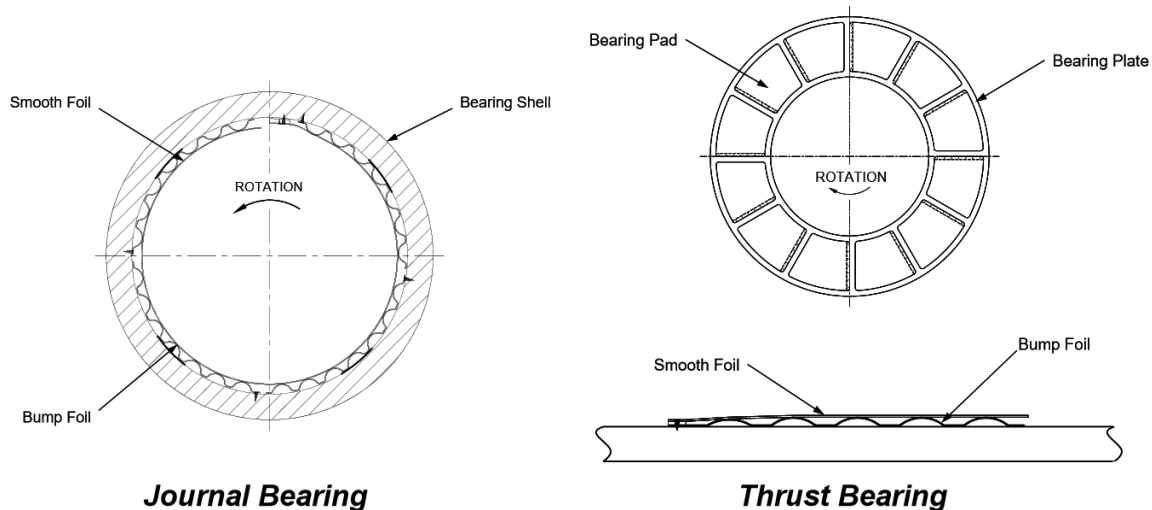


Figure 3. Typical construction for bump foil journal and thrust bearings ^[3]

2.3. Bearings for S-CO₂ Power Systems

Turbomachinery for S-CO₂ power systems presents unique challenges to bearing support systems resulting from the working fluid properties of S-CO₂. It has significantly higher fluid density and lower density than conventional working fluids. This combination results in compact, power-dense, turbomachinery which presents unique challenges relating to bearing surface speed and bearing unit load.

A variety of bearing types can be considered for S-CO₂ systems. A summary of the different bearing types considered for use in S-CO₂ applications and their relevant power ranges is given in Figure 4. The ones most commonly considered are ^[3]:

- (1) Gas Foil Bearings
- (2) Magnetic Bearings
- (3) Hydrostatic (CO₂ Liquid or Gas) Bearings
- (4) Hydrodynamic (CO₂ Liquid or Supercritical Fluid) Bearings
- (5) Hydrodynamic (Oil Lubricated Tilt-Pad) Bearings
- (6) Hydrodynamic (Oil Lubricated Roller or Elliptical) Bearings

Large industrial sized power plants rely primarily on hydrodynamic oil tilting pad bearings for both the thrust and journal loads. Some consider these the most likely candidate for future large scale S-CO₂ systems ^[2,3]. The advantages that they have over the others for future S-CO₂ technology,

is that they are commercially available from a variety of OEMs, they are rotor dynamically stable, able to withstand high axial and radial loads, and can operate at shaft speeds up to 30,000-40,000 rpm on the small-diameter shafts needed for pilot plants in the 10MWe power range. The use of these bearings in S-CO₂ systems leverages the significant industrial investment in this technology, and confirms that standard industrial seals and buffer gas management systems can be used with minimal loss in this application.

The other bearing types (gas foil bearings, magnetic bearings, hydrostatic bearings, and hybrid bearings) are useful primarily for S-CO₂ R&D test facilities. These offer potential advantages that include simplified sealing systems, higher operating speeds, and longer shafts by placing the bearing midway along the length of a multi-staged turbomachine. Disadvantages with these include design challenges such as complicated rotor dynamics, high windage, and heating with requirements for local cooling. An additional disadvantage is the lack of history with these bearings in the power industry, whereas there is a long history with the oil bearings.

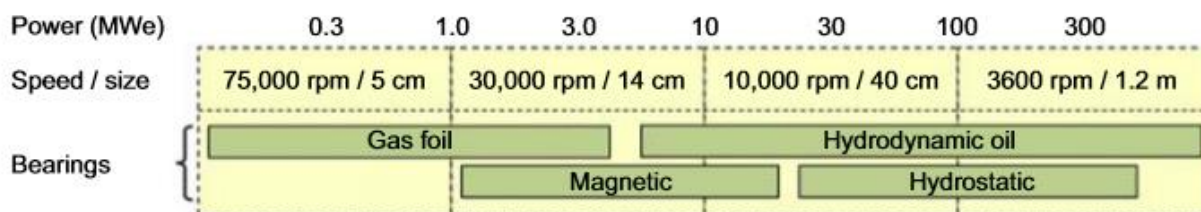


Figure 4. Types of bearings proposed for use in S-CO₂ applications across range of rotor power ^[2]

The landscape of S-CO₂ power systems development includes the development and use of a variety of these bearing approaches. Research teams in Korea (KAIST ^[4] and KIER ^[5]) used gas foil bearings in a 100kWe test loop, oil lubricated tilt-pad bearings in a 80kWe system, and magnetic bearings in a turbopump. For the GE/SWRI collaboration under the SunShot program, oil lubricated tilt-pad journal bearings were used in their 10MWe prototype system ^[2]. Barber-Nichols has advocated for the use of S-CO₂ hydrostatic bearings as an alternative to traditional hydrodynamic bearings ^[6]. They describe the performance of S-CO₂ hydrostatic bearings exceeding most other bearing technologies in load capacity, stiffness, and damping. The principal disadvantages for these are their cost, complexity, and inefficiency of using an external supply. Companies that design and build bearings have described ongoing work to develop porous externally pressurized gas bearings ^[7] and advanced gas foil bearings ^[3] for S-CO₂ turbomachinery. For the 250kWe S-CO₂ test system at Sandia, gas foil bearings were developed for both radial and thrust support ^[8]. More details for the bearing technology used in this system is described in the next section of this report.

2.4. Sandia RCBC System

During the development of the Sandia S-CO₂ system turbomachinery, a thorough analysis of all bearing options was completed ^[8]. Primarily, it was clear that bearings would have to operate within a CO₂ environment, as adequate rotating seals for S-CO₂ simply did not exist to allow bearings to operate outside the pressurized system. This eliminated more traditional approaches

that would have isolated bearings from the process fluid, and used oil-lubricated bearings. In some sense, this simplified the system from dependency on cumbersome ancillary equipment for pumping, storing, cooling, sealing, plumbing, and filtering the oil lubricant. Furthermore, oil cannot sustainably lubricate a system at high temperatures, due to thermal breakdown. Magnetic bearings would have required a more complex development effort, and were temporarily set aside from consideration. Ball bearings had been tested in S-CO₂ during the seals development process, but did not perform well, requiring frequent replacement. Over time, the poor viscosity of CO₂ allowed the rolling elements to come into more aggressive contact than they would in oil, resulting in rapid wear and deformation.

This left gas foil bearings, which in contrast make use of the process working fluid to generate a hydrodynamic load capacity that increases with speed, eliminating system contamination from oil and enabling higher temperature operation. Compliance in the structural foils allows the bearings to deform under load for increased capacity, and to compensate for misalignment and distortion. The main disadvantages with these were mainly centered around the lack of experience in high pressure CO₂ film lubrication environments. Questions centered on the amount of friction that would be generated, maximum load capacities that would be supported, and rotordynamic stiffness of the gas lubricant system.

Thus, the Sandia S-CO₂ RCBC loop Turbine-Alternator-Compressor (TAC) was developed utilizing a series of gas foil bearings. Radial (or Journal) bearings are located at both the turbine and compressor sides of the TAC, while the compressor side also has an axial (or thrust) bearing. Each bearing operates in an environment of around 300 psi CO₂. The turbine-side radial bearing is at a significantly higher temperature (~ 550°C) than at either of the compressor-side bearings (~ 315°C). The locations for each bearing are shown in Figure 5.

The journal bearings were obtained off-the-shelf from Capstone. These are approximately 2" long and 1.5" in diameter and have different solid lubricant coatings for the turbine and compressor sides of the TAC. The high temperature turbine side journal bearing uses a patented Capstone coating material with an upper temperature limit of 538°C (1000°F), while the compressor end journal bearing uses a Teflon-based coating capable of reaching temperatures of 232°C (450°F). In both cases the foil themselves are made from Inconel X750. Several images of these gas foil journal bearings are shown in Figure 6.

Design uncertainties for foil journal bearings were minor compared to those for the foil thrust bearings. No commercial manufacturer was identified to deliver a foil thrust bearing, therefore they were designed and built in-house at Barber-Nichols from open source information provided by NASA Glenn Research Center. Based on NASA's experience, a foil thrust bearing was developed which was 4" outer diameter, 2" internal diameter, and featured 6 pads. The foils themselves were made from Inconel X750, and a Teflon coating was applied as the foil coating material. Several images of a gas foil thrust bearing are shown in Figure 7.

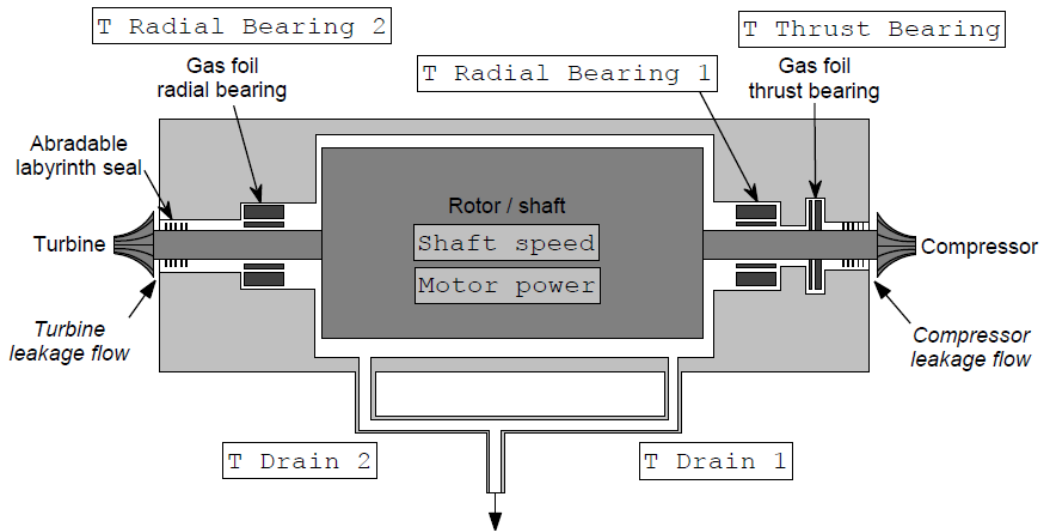


Figure 5. Diagram of Sandia's S-CO₂ TAC showing the location for the bearings

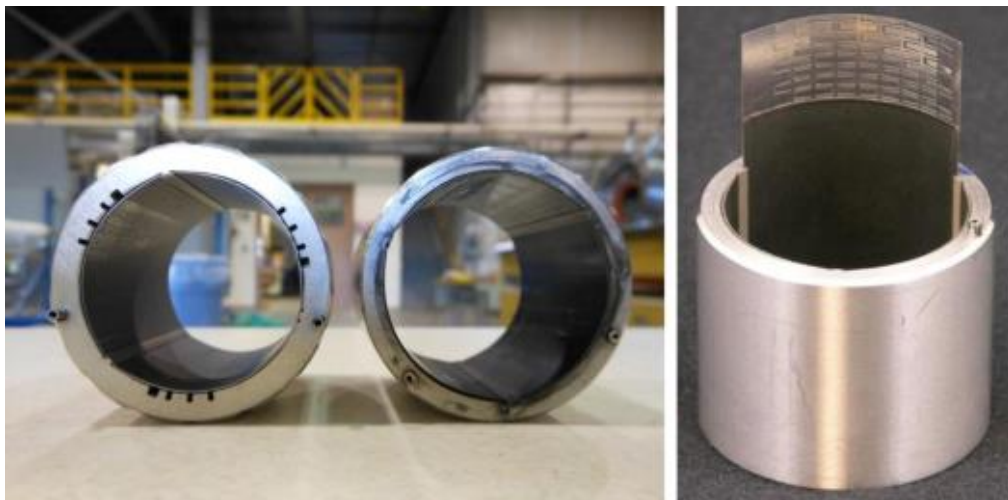


Figure 6. Images of the gas foil radial (journal) bearings used in Sandia's S-CO₂ RCBC loop



Figure 7. Images of the gas foil axial (thrust) bearing used in Sandia's S-CO₂ RCBC loop

2.5. Identified Research Needs for S-CO₂ System Gas Foil Bearings

Information regarding the performance of gas foil bearings has been gleaned through their short duration operation in the Sandia S-CO₂ RCBC during the past several years. The journal bearings have appeared to work adequately; while there have been significant challenges with the thrust bearings. In fact, thrust bearings have been identified as a limiting issue in S-CO₂ turbomachinery development for small-scale hardware ^[8]. Consensus is that the Teflon coating appears inadequate for the temperatures in which this bearing operates, and there is a need for hardware that is capable of sustaining higher temperatures during operation.

While the journal bearings have appeared to work well, they have challenges of a different nature. The company that makes these, Capstone, no longer sells their journal bearings. An alternative source for journal bearings is currently needed, with the complication of not knowing the high temperature coating material that Capstone was using on their versions of turbine-side journal bearings.

Collectively, these issues prompted the need to initiate an investigation to evaluate and identify alternative foil coating materials for these bearings. Two areas of research at Sandia are focused on addressing this. One, is the establishment of a bearing test rig for conducting tests of advanced bearing designs separate from the RCBC test loop. Once commissioned, this will be used for evaluating vendor supplied bearing performance under conditions relevant to S-CO₂ RCBC operation, including cyclical start-stop testing to assess the tribological properties for the bearing coating materials.

The second area, which is the topic for this report, is the evaluation of foil coating materials themselves in relevant pressure/temperature environments to actual bearings. These will be valuable in screening vendor supplied foils for use in future gas foil bearing rig tests, in addition to providing a baseline of behavior for some of the currently used foil materials. Very little is actually known about the behavior of foil coating materials in the high temperature/pressure CO₂ environment of these bearings, and there is tremendous value to obtaining this information in a manner independent of mechanical loads.

3. Approach

An experimental program was initiated to elucidate the behavior of coated bearing foil materials in the harsh environments of the Sandia RCBC system. The overall approach to this work involved the following main activities: (1) Collaborating with gas foil bearing vendors to identify candidate foil coating materials to be tested, (2) Acquiring samples of the various coating materials in formats relevant to use in an actual RCBC system, (3) Developing an appropriate test configuration for completing the evaluations, (4) Identifying appropriate sample characterizations that are relevant to coating material performance within a gas foil bearing, and (5) Completing a series of long duration exposure tests (500hr) along with the appropriate post-test sample characterizations. Details are provided in each of these areas in this section of the report.

3.1. Identification of Candidate Foil Coating Materials

The starting point for conversations with gas foil bearing vendors regarding foil coating materials, was the operating environment (pressure and temperature) for the various bearings within the TAC. Analysis by members of the Sandia S-CO₂ team in Albuquerque, NM established a pressure of 300 psi CO₂ at both the turbine-side and compressor-side bearings. Additionally, a temperature of 550°C was established for the turbine-side bearings, and a temperature of 315°C was established for the compressor-side. Using this information, bearing vendors were able to identify a variety of candidate materials for these evaluations. In some instances, candidate materials were identified to be evaluated at only one of these two conditions (315°C or 550°C), while in others materials were identified to be evaluated at both.

Three vendors were approached to collaborate on this project: (1) Xdot Engineering and Analysis of Charlottesville, VA, (2) Mechanical Solutions of Albany, NY, and (3) Mohawk Innovative Technology of Albany, NY. Two of these vendors, Mohawk Innovative Technologies and Mechanical Solutions, Inc., expressed concern over the public release of their coating chemical formulation associated with the analyses as part of this program. An NDA was established with Mechanical Solutions, Inc., that will protect their coating chemical formulation from public release. The same could not be done with Mohawk Innovative Technologies, and unfortunately they decided to withhold samples from these tests. In the case of Xdot, there were no issues. They differ a bit from the others, as they are more focused on bearing design rather than on developing coating materials themselves.

Besides evaluations of newly identified coating materials, inclusion of samples that have the current coatings used in Sandia's test loop bearings is important as a comparison. This establishes a baseline of performance, against which to compare the other options being evaluated. Unfortunately, only samples with the low temperature compressor-side thrust bearing coating were included, as the supplier for the other bearings (Capstone Turbines) was unwilling to provide samples for these tests.

3.1.1. Xdot Engineering and Analysis

Xdot worked with four separate coating vendors to provide a series of 6 different coatings for evaluation. Being involved in bearing design, it was very important to Xdot that the coating be evaluated in the format that it will be used in a real bearing. To achieve this, they provided samples for each of the coatings across a range of possible formats. The different sample formats included flat foil, rolled or curved foil, and cylindrical; these are shown in Figure 8. In each case the coating material was applied to the sample surface. The flat foils were included to represent the thrust bearing foils, while the curved foils represent those for the journal bearing. The cylindrical samples represent a case where the coating is applied to the rotating shaft itself rather than to the bearing foils.

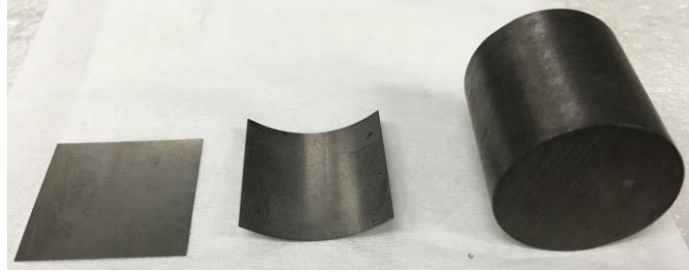


Figure 8. Sample formats used for gas foil bearing performance evaluations

One of the coating vendors was Everlube Products (Peachtree City, GA), which is a business unit of Curtiss-Wright. Two of their solid film lubricant materials, Perma-Slik RMAC and RWAC, were evaluated at both of the exposure conditions in both the flat foil and curved foil sample formats. The foil substrate material for these samples was 1" x 1" Inconel X750. The RMAC product uses molybdenum disulfide (MoS_2) as the solid lubricant, while the RWAC product uses tungsten disulfide (WS_2).

A second coating vendor was General Magnaplate (Linden, NJ). Two of their Nedox 10K coatings, 10K2 and 10K3, were evaluated in both the flat foil and curved foil sample formats. The foil substrate material for these samples was 1" x 1" Inconel X750. The 10K2 material was evaluated only at the higher temperature exposure condition, while the 10K3 was evaluated only at the lower temperature condition. Both materials appear to use primarily nickel in the coating.

TURBOCAM International (Dover, NH) was a third coating vendor. Their TX1 surface treatment differed versus all of the other materials investigated, as this was not a coating, but rather a metal surface treatment process (nitride) imposed on the surface. Two images are shown in Figure 9 for this surface treatment; the image on the left is a microscope image for the material surface cross-section and on the right is an EDS map of nitrogen for the same cross-section area. This shows the presence of nitrogen at the sample surface area, which imparts hardness, wear resistance, and lubricity to the surface. TX1 was evaluated at both of the exposure conditions in all three sample formats. The substrate material was now 1" x 1" 316 stainless steel rather than Inconel X750, due to the requirements for the surface treatment process. For both the flat and curved foil samples, samples were evaluated for three separate vendor applications of the surface treatment. These samples are designated as treatments A, B, and C, and the parameters of the surface treatment process differed slightly among the three.

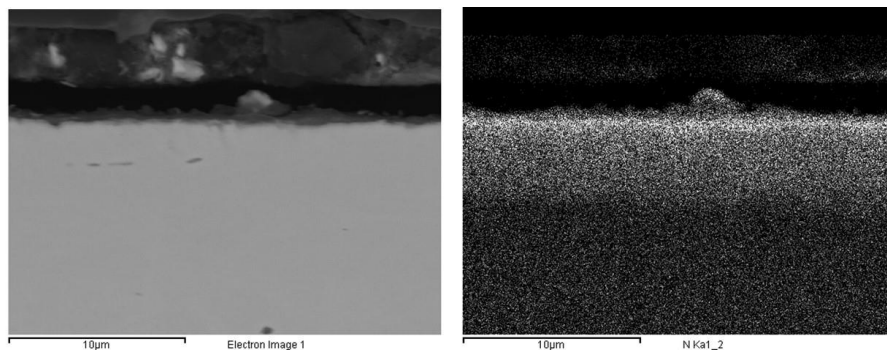


Figure 9. SEM images of a sample with the TX1 nitride surface treatment

A final coating was the NASA developed PS400 material, which is provided by Hohman Plating and Manufacturing (Dayton, OH). This material, being applied to the metal surface by plasma spray, was provided onto thicker metal substrates (0.125") of 1.25" x 1.25" 15-5 stainless steel. In an actual bearing application, it would likely be applied to the thrust runner disk surface or shaft, rather than to the bearing foils. It was evaluated in this thicker plate format at both of the exposure conditions. PS400 is the latest in a long line of plasma-sprayed solid lubricant coatings dating back to the 1970s, all developed at NASA Glenn Research Center^[9,10]. It is comprised of a nickel-molybdenum-aluminum binder with added chromium oxide, silver, and barium-calcium fluoride. The silver and barium-calcium-fluoride (5% by mass) provide the solid lubrication, while chromium oxide (25%) is used as a hardener, and nickel-moly-aluminum (70%) is tough binder matrix to stabilize the solid layer. A coating cross-section chemical analysis for this material is shown in Figure 10. Compared to the previous generation coating PS304, it has higher density, smoother finish, better stability, good creep resistance, strength, oxidative and dimensional stability. Solid lubricant content was halved from 10wt% to 5 for PS400 as compared to its predecessor. Total coating thickness of at least 300 μm , is built up layer by layer in many separate plasma spray passes.

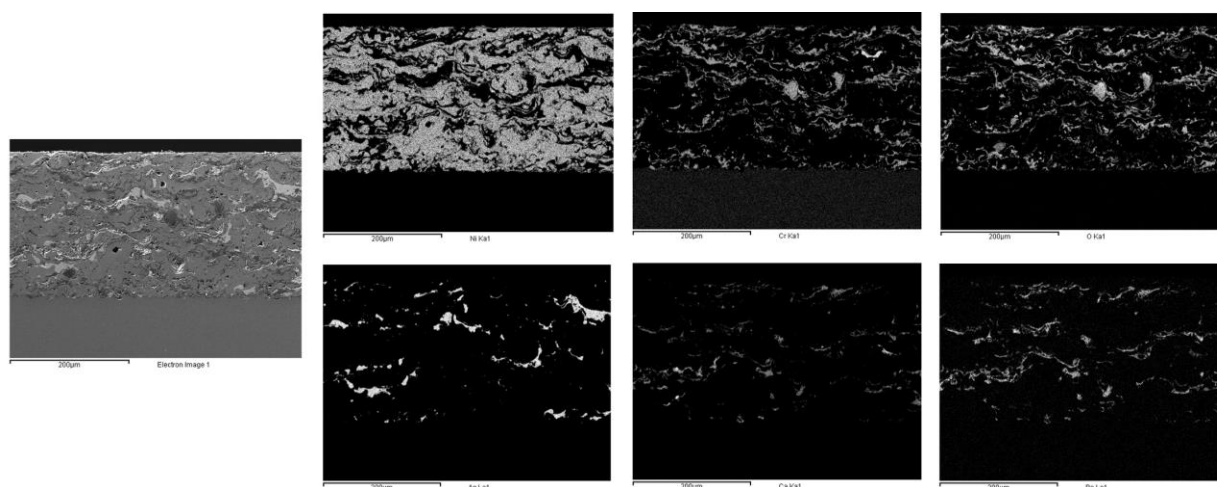


Figure 10. EDS chemical analysis for the PS400 coating

3.1.2. Mechanical Solutions

It is unclear if Mechanical Solutions worked with a coating vendor to develop their gas foil bearing coating materials, or whether they have developed these internally. They did not provide any information on their coating materials, as this is a sensitive technology to their business that they would like to protect. The chemistry of their coating materials will not be disclosed as part of this report, but instead the performance of these materials will be compared to the others included in this study.

Samples with three different coating materials were provided for these evaluations; these were labeled by the vendor as A39, A40, and A42. The differences between these three materials were not disclosed, and so these will be treated separately as three separate coating options.

These were provided in the 1" x 1" flat foil format only, and the substrate material was Inconel X750. All of the samples were evaluated at both sets of exposure conditions.

3.2. Exposure Furnace Setup

The test configuration for these evaluations was established using the high temperature autoclave furnace that was used previously for the carbon steel S-CO₂ corrosion study^[11]; this is located at the laboratory in Livermore, CA. The furnace itself was modified to allow for tests in a controlled atmosphere of 300 psi CO₂, instead of in S-CO₂. While the pressure is maintained at 300 psi, the setup allows for a flow of fresh CO₂ through its chamber. Temperature of the internal chamber is measured across its length in three locations. A photo of the furnace setup for these tests is shown in Figure 11.



Figure 11. Modified autoclave furnace for gas foil bearing tests at 300psi CO₂

A new sample holder approach was designed for use in these experiments. This was an important aspect to this work, as there were many different sample types and formats to include in each of the tests; each test included over 60 samples. The approach that was developed involved the use of an aluminum oxide ceramic platform (D-Tube), on which the samples were oriented using machined aluminum oxide ceramic sample holders. Samples were oriented within the holders using machined notches spaced along their length. In the case of the thicker samples (PS400) and cylindrical samples, these were placed directly onto the ceramic platform rather than in a machined sample holder. The photos in Figure 11 show how the holder was utilized for the curved foil (A) and flat foil (B) samples, while the photo in Figure 12 shows how the holder was utilized for the full suite of samples in a single test. The dimensions for the holder were 13" long and 1.5" wide, and the height was such that the samples were positioned at the vertical center of the furnace.

Two long duration exposure experiments were performed using this setup, covering the two exposure conditions relevant to bearing foil materials. In one test, an exposure temperature of 550°C was used to mimic the conditions for the turbine-side journal bearings. In a second test, a temperature of 315°C was used to mimic the conditions for the compressor-side journal and thrust bearings. In each test, the total exposure duration was 500 hours, which is significantly longer than has been achieved previously for bearing foil materials in these environments. Industrial grade CO₂ was used for both experiments in order to mimic the conditions inside of a bearing that would be used in a real system.

Four samples of each coating material and sample format were included into each of these exposure experiments. This was done to be able to provide samples for the various post-test analyses that are described in the next section of this report. Also, having multiple samples of each coating material/sample format adds reliability to the data from these experiments instead of basing all of the analyses / results off of a single sample.

Information for each of the coating materials investigated through this set of experiments are summarized in Table 2. Pertinent information for the materials from both Xdot and Mechanical Solutions are included, along with the available information for the “baseline” bearing materials currently used in the Sandia RCBC system. Images for each of the sample types included in the higher temperature exposure test (550°C) are shown in Figure 14, while images for those included in the lower temperature test (315°C) are shown in Figure 15. In the case of the samples in the top two rows, samples are shown in both the flat (top) and curved (bottom) formats.

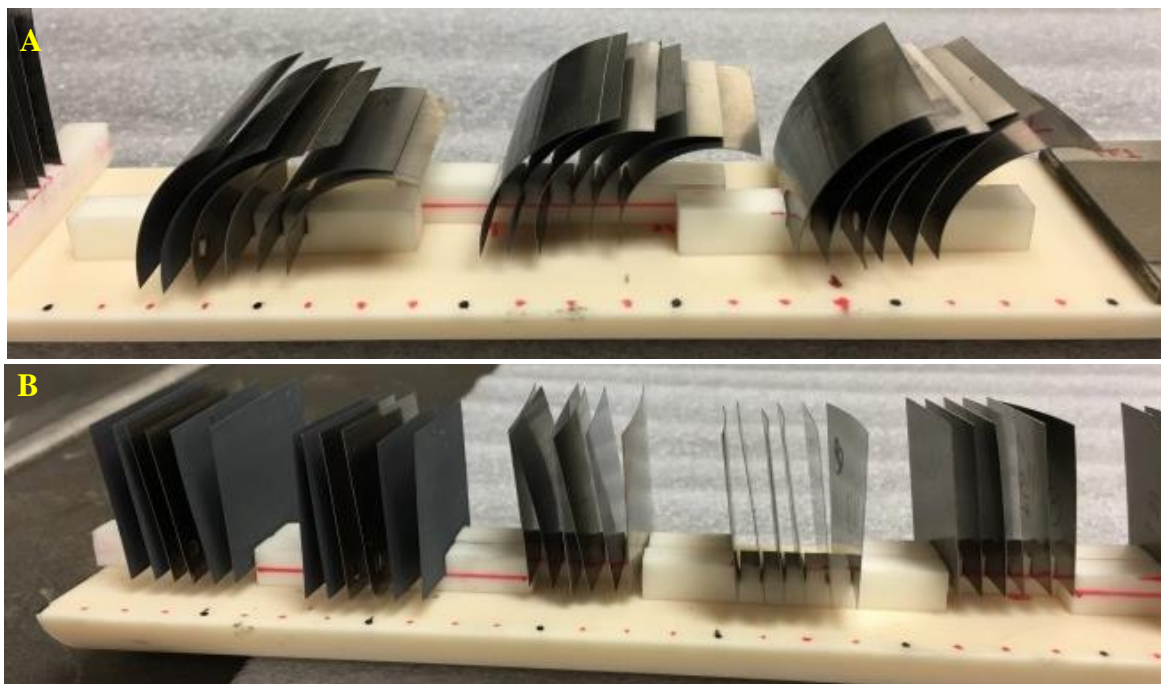


Figure 12. Sample holder configuration used for curved foil samples (A) and flat foil samples (B)



Figure 12. Sample holder loaded up with the full complement of samples for an exposure test

Table 2. Descriptions of Bearing Foil Coating Materials

Sample Name	Bearing Vendor	Coating Vendor	Coating Name	Coating Mtl	Coating Thickness (microns)	Substrate Alloy	Turbine, Compressor, Both
MoS ₂	Xdot	Everlube	Perma-slik RMAC	MoS ₂	10-16	X750 Inconel	Both
WS ₂	Xdot	Everlube	Perma-slik RWAC	WS ₂	30	X750 Inconel	Both
10K2	Xdot	General Magnaplate	Nedox 10K2	Ni-P and Si-O	7-8	X750 Inconel	Turbine
10K3	Xdot	General Magnaplate	Nedox 10K3	Ni-P and Si-O	13-23	X750 Inconel	Compressor
TC A	Xdot	TurboCAM	TX1 (Treatment A)	Nitride Surface Treatment	n/a	316 ss	Both
TC B	Xdot	TurboCAM	TX1 (Treatment B)	Nitride Surface Treatment	n/a	316 ss	Both
TC C	Xdot	TurboCAM	TX1 (Treatment C)	Nitride Surface Treatment	n/a	316 ss	Both
PS400	Xdot	Hohman Plating (NASA)	PS400	NiMoAl, Cr-oxide, Ag, Ba-Ca fluorides	380-500	15-5 ss	Both
A39	Mechanical Solutions	Mechanical Solutions	A39	n/a	1.50	X750 Inconel	Both
A40	Mechanical Solutions	Mechanical Solutions	A40	n/a	1.50	X750 Inconel	Both
A42	Mechanical Solutions	Mechanical Solutions	A42	n/a	1.50	X750 Inconel	Both
Baseline-Thrust	SNL	Barber-Nichols Inc.	Unknown	Teflon	20-22	X750 Inconel	Compressor
Baseline-Journal (LT)	SNL	Capstone Turbines	Unknown	Teflon	n/a	X750 Inconel	Compressor
Baseline-Journal (HT)	SNL	Capstone Turbines	Unknown	Unknown	n/a	X750 Inconel	Turbine

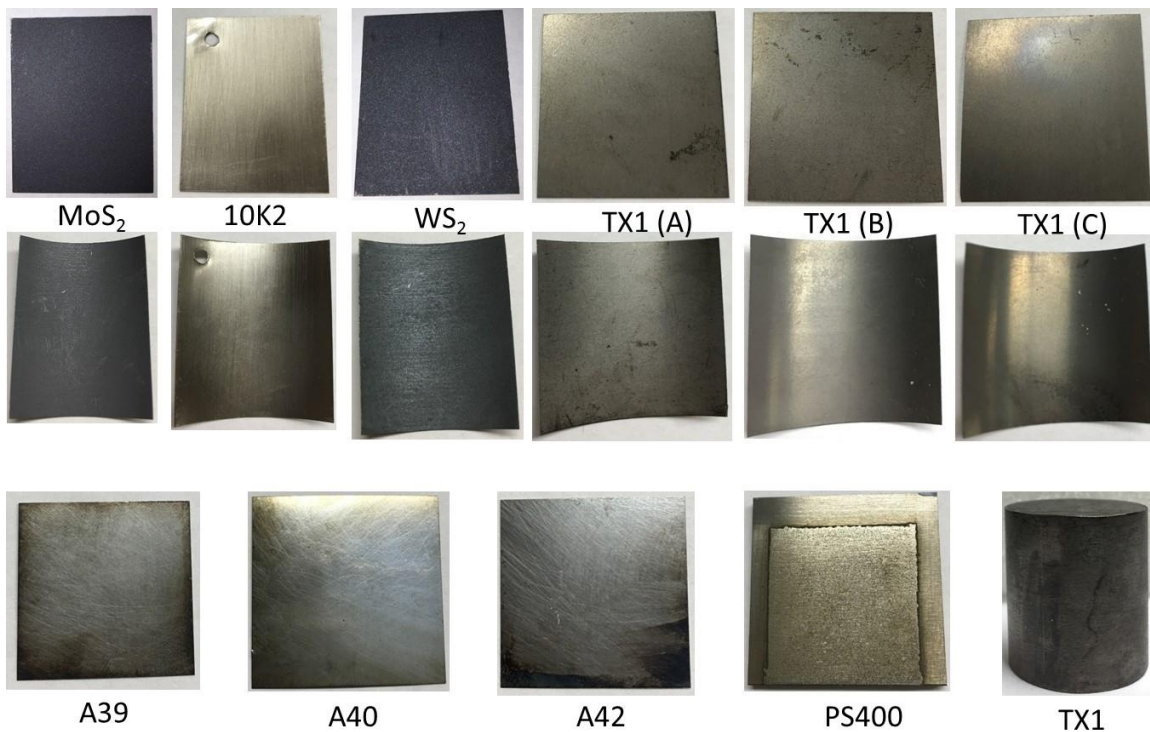


Figure 14. Sample types included in the higher temperature (550°C) exposure test

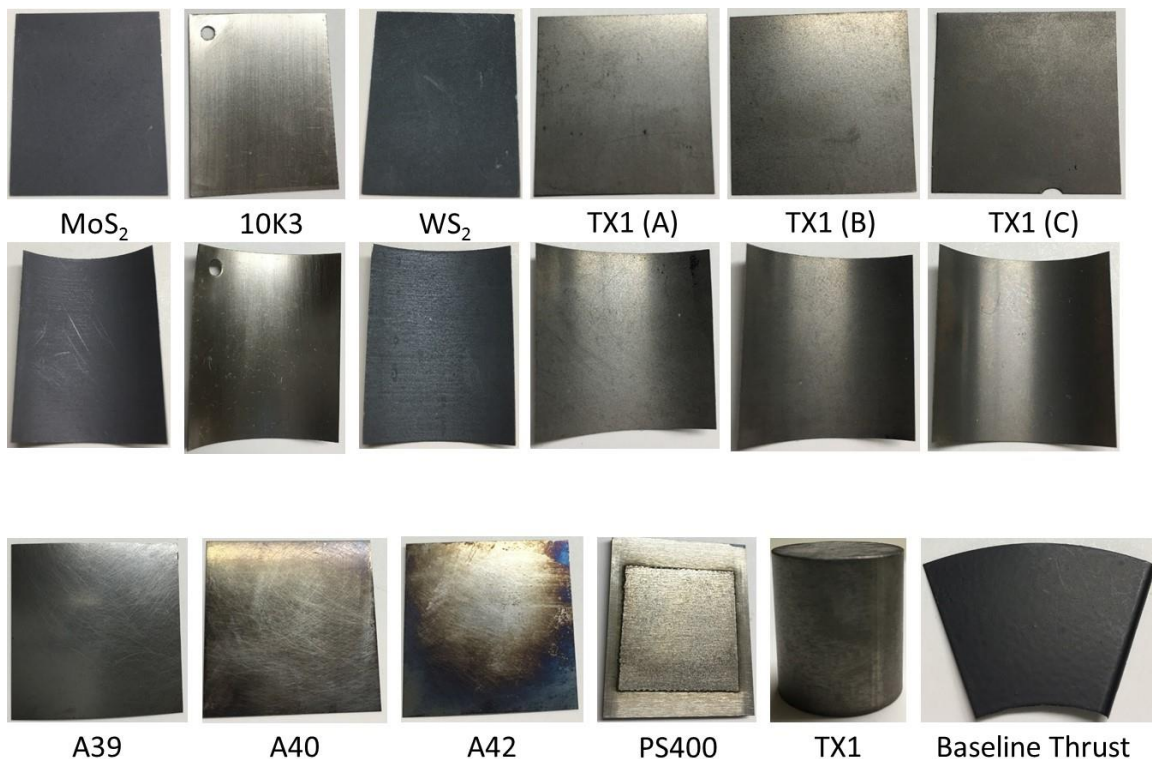


Figure 15. Sample types included in the lower temperature (315°C) exposure test

3.3. Test Sample Characterization

The approach to sample characterization was focused around understanding the chemical compatibility of the materials with its environment, and how these interactions may influence the materials performance as a bearing foil coating. Conversely, understanding and characterizing the tribological properties of the coating materials in their use environments was not the focus. Through discussions with the participant bearing vendors, it was determined that the tribological performance for these materials would be best characterized through start-stop testing in the future bearing-test rig, as these properties need to be measured as the material is being used in its intended environment. Along this vein, the characterizations identified for these exposure tests were intended as a screening tool to identify candidate coating materials for further evaluations in the bearing-test rig.

The main areas of sample characterization included in this investigation included visual observation of samples for coating spallation, weight change measurements to identify material oxidation or evaporation, microscopic examination of the coating/substrate microstructure, surface roughness measurements, and scratch testing to reveal a variety of parameters around the durability of the coating material. These areas were determined through conversations with subject matter experts internal to Sandia as well as those external (NASA, Xdot, and Mechanical Solutions). Details are provided for each of these areas of sample characterization in the following sections.

3.3.1. Visual

A digital camera was used to capture images for bearing foil samples both before each test as well as after 500 hours environmental exposure. These are useful to capture information about how coating surfaces change resulting from exposure to CO₂ and temperature, as well as differences that may exist from one temperature to the other. These images also capture any coating spallation that has occurred during the exposure; important information to pair with weight change measurements in order to distinguish degradation mechanisms as either coating evaporation from spallation.

3.3.2. Weight Change

Sample weight change, resulting from the 500 hour environment exposures, were measured using a Mettler-Toledo XP-26 Microbalance. Measurements were made for all samples in each of the two exposure experiments. The coating material, as well as the alloy substrate material, may react with the CO₂ environment during exposure. Weight change measurements can provide valuable information about these interactions.

Sample weight gain is indicative of sample oxidation. While this can result from reactions between the coating material and CO₂, this is most likely attributed to oxidation of the alloy substrate. Substrate oxidation can occur if the coating material is porous to the CO₂ environment, and this is undesirable as this can degrade the coating/substrate interface integrity. It can also decrease the lifetime for the bearing foil material as the substrate material is degraded.

The opposite scenario, sample weight loss, can also be a concern as this indicates either coating spallation or coating evaporation. The aforementioned visual characterization of the samples can help to differentiate between the two. Both are undesirable, as this indicates instability of the bearing materials in the use environments. These will ultimately decrease the lifetime for the bearing foil, and in the case of spallation, also for the bearing itself due to the resulting particulate abrasion that would likely occur.


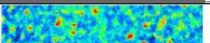
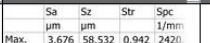

3.3.3. Coating/Substrate Microstructure

Environmental exposure of the samples can cause microstructural changes to the coating material itself or to the coating/substrate interface. These are important to characterize and understand for each of the candidate coating materials. Microstructural changes of the coating material can contribute to changes in other sample characteristics such as surface roughness, damage resistance, and adhesion strength to the substrate. Changes to the coating/substrate interface, possibly caused by oxidation reactions with the CO₂ environment, can influence the coating adhesion strength to the substrate.

For each sample type, one specimen was characterized for microstructural changes. This was done for samples in the pre-exposed condition, as well as for after each of the two exposure conditions, so that comparisons could be made among the three conditions (no exposure, 500hrs

3.3.4. Surface Roughness

Surface roughness measurements were completed for two flat foil samples of each type. Measurements were completed for samples prior to exposure, followed by repeat measurements on the same exact samples following the completion of the exposure experiments. Three measurements were made in different areas on each sample. Measurements were completed using a Keyence VK-X Series 3D Laser Scanning Confocal Microscope, which provides non-contact, nanometer-level profile and roughness measurements.

File name	Surface roughness		Main image	Surface roughness		Surface roughness	Surface roughness	Surface roughness	Surface roughness	Surface roughness	3D image																																		
	Original surface	Laser+Optical		Measured values	Area1	Area1	Area1	Area1	Area1																																				
					Sa	Sz	Str	Spc	Sdr																																				
		Height				μm	μm		1/mm																																				
170117_ap-i-140_WIS2_A1				<table border="1"> <thead> <tr> <th></th> <th>Sa</th> <th>Sz</th> <th>Str</th> <th>Spc</th> </tr> <tr> <th></th> <th>μm</th> <th>μm</th> <th></th> <th>1/mm</th> </tr> </thead> <tbody> <tr> <td>Max.</td> <td>3.676</td> <td>58.532</td> <td>0.942</td> <td>2420</td> </tr> <tr> <td>Min.</td> <td>3.676</td> <td>58.532</td> <td>0.942</td> <td>2420</td> </tr> <tr> <td>Ave.</td> <td>3.676</td> <td>58.532</td> <td>0.942</td> <td>2420</td> </tr> <tr> <td>Std. DV</td> <td>0.000</td> <td>0.000</td> <td>0.000</td> <td>0</td> </tr> <tr> <td>Area1</td> <td>3.676</td> <td>58.532</td> <td>0.942</td> <td>2420</td> </tr> </tbody> </table>		Sa	Sz	Str	Spc		μm	μm		1/mm	Max.	3.676	58.532	0.942	2420	Min.	3.676	58.532	0.942	2420	Ave.	3.676	58.532	0.942	2420	Std. DV	0.000	0.000	0.000	0	Area1	3.676	58.532	0.942	2420	3.676	58.532	0.942	2420.362	2.026	
	Sa	Sz	Str	Spc																																									
	μm	μm		1/mm																																									
Max.	3.676	58.532	0.942	2420																																									
Min.	3.676	58.532	0.942	2420																																									
Ave.	3.676	58.532	0.942	2420																																									
Std. DV	0.000	0.000	0.000	0																																									
Area1	3.676	58.532	0.942	2420																																									

M3AT-17SN1906025

3.3.5. Scratch Testing

The scratch resistance and adhesion strength of coating materials can be determined using the instrumented scratch testing method. In evaluating bearing foil coating materials these are important parameters to understand between the various coatings as well as for the same material as a function of environmental exposure. The foil coating material should be resistant to damage (scratching, etc.) and have strong adherence to the metal substrate; both are important to avoiding debris generation within the bearing as well as maintaining the low friction coating surface for periods of operation where rubbing occurs.

In this test method, a diamond stylus of defined geometry is drawn across the flat surface of a coated test specimen at a constant speed and defined normal force (progressively increasing) for a defined distance. The damage along the scratch track is microscopically assessed as a function of the applied force. This technique is able to differentiate between cohesive failure within the coating (coating scratch damage resistance) and adhesive failure at the interface of the coating-substrate system (coating adhesion strength).

This test method is illustrated in Figure 17. Here, several pieces of information are brought together to demonstrate the method. The drawing at the top illustrates the damage that occurs to the coating material as the stylus moves across the surface. The two types of coating failure, cohesive and adhesive, are indicated here. Below this is a microscopic image of the sample surface. Again, the two distinct types of coating failure are indicated. The visual differences between these types of failure are used to indicate when these occur for a test sample. Finally, at the bottom is a chart indicating the applied normal force (blue), the resulting frictional force (green) and stylus penetration depth (red) across the length of the scratch. The microscopic image together with the chart are used to identify the force at which the two types of failure occur for a sample.

Flat foil samples of each type for each environmental exposure condition were sent out to EP Laboratories in Irvine, California for instrumented scratch testing. Unexposed flat foil samples of each type were also sent for testing. Testing was completed in triplicate for each sample, and followed the relevant ASTM Standards (G171, C1624, and D7187). The test conditions and parameters used for tests are provided in Table 3.

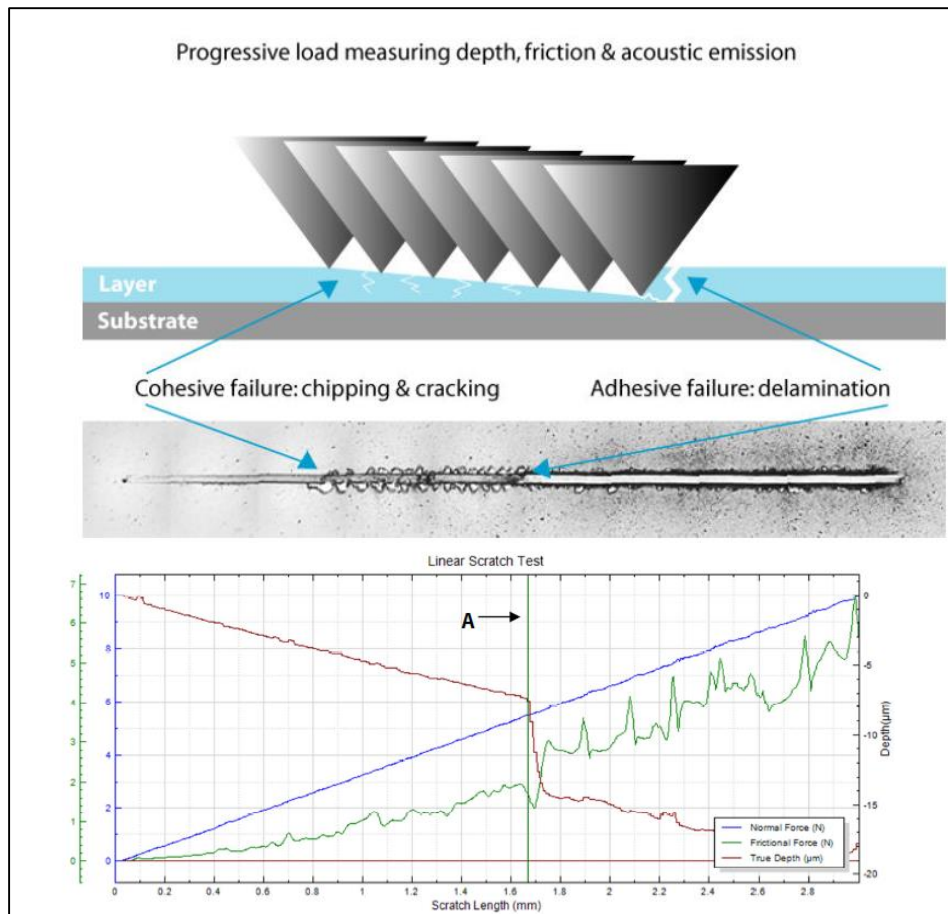


Figure 17. Illustration of multiple elements to instrumented scratch testing

Table 3. Test Conditions and Parameters used for Instrumented Scratch Testing

Load Type	Progressive
Initial Load	3 mN
Final Load	500 mN
Scanning Load	3 mN
Loading Rate	500 mN/min
Scratch Length	1 mm
Speed	1 mm/min
Distance between scratches	1 mm
Cantilever	HL-125
Indenter	Rockwell Diamond Radius 10 μm ID: SD-A33/90
Indenter Source	CSM Instruments
Indenter Inspection	Indentation in Copper Before and after testing samples
Temperature	21-23°C
Relative Humidity	45-48%
Conditioning	21-23°C for minimum 24h

4. Results

Sample characterization included visual observation of samples for coating spallation, weight change measurements to identify material oxidation or evaporation, microscopic examination of the coating/substrate microstructure, surface roughness measurements, and scratch testing to reveal a variety of parameters around the durability of the coating material. Results are presented for coating materials in each of these areas for the two separate 500 hour exposure experiments.

4.1. Visual

The newly developed sample holder was found to work well for both exposure experiments, allowing for a large number samples of different formats in each test. Photos were taken of the samples on the holder after being removed from the autoclave furnace. These are shown for the two experiments in Figure 18. For the higher temperature exposure (550°C), the most notable observation was the spallation for some of the curved foil samples. This was only observed for the samples with the TX1 surface treatment, and only for the samples in the curved foil and cylinder formats. In the case of the lower temperature test (315°C), the most notable visible feature was the cracking observed for the Baseline Thrust Bearing flat foil sample.

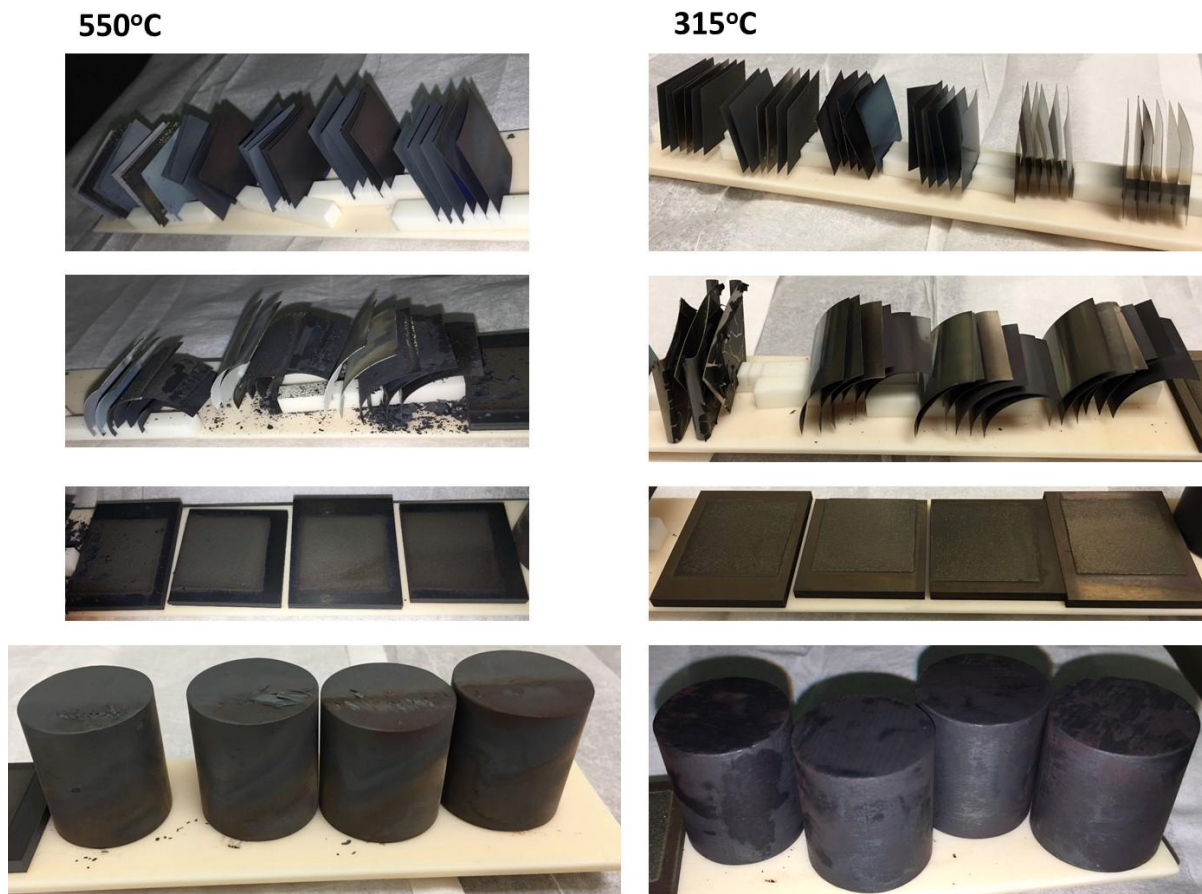


Figure 18. Samples on the holder following the two exposure experiments (550°C and 315°C)

Images for each of the sample types are compared pre- and post- exposure. For each of the exposure tests, these are broken out into two separate groups. In one group are all of the flat foil samples for that particular exposure condition, while in the other group, are all of the alternative format samples (curved, thicker flat, and cylinder). The samples from the lower temperature exposure test are shown in Figure 19 and Figure 20, while those for the higher temperature test are shown in Figure 21 and Figure 22.

The sample appearances were observed to change very little following the lower temperature exposure. The samples with the TX1 surface treatment appeared to be darker following the test, resulting from surface oxidation. The Mechanical Solutions samples (A39, A40, A42) had a bluish surface coloring after exposure that was not present prior to this. The Baseline Thrust Bearing foil sample showed the most significant change following the exposure test. The surface was found to have formed many very large cracks, with areas of coating delamination. These have not been observed previously in the operation of the Sandia RCBC, and so this may indicate that the exposure test temperature of 315°C is higher than the actual case in the RCBC system compressor thrust bearing. Lastly, nothing really stood out about the curved sample formats in this test versus those in the flat format.

Following the higher temperature exposure, sample appearances were observed to change more dramatically. The one exception being the PS400 sample, which only appeared slightly darker than in the pre-exposed condition. The most concerning of the changes was observed for the TX1 samples, where significant surface oxidation was observed, along with extensive spallation for those with the curved surfaces. While other types of samples had modified surface coloring after the exposure, all of the coatings appeared to remain intact on the foil samples without obvious cracking and spallation.

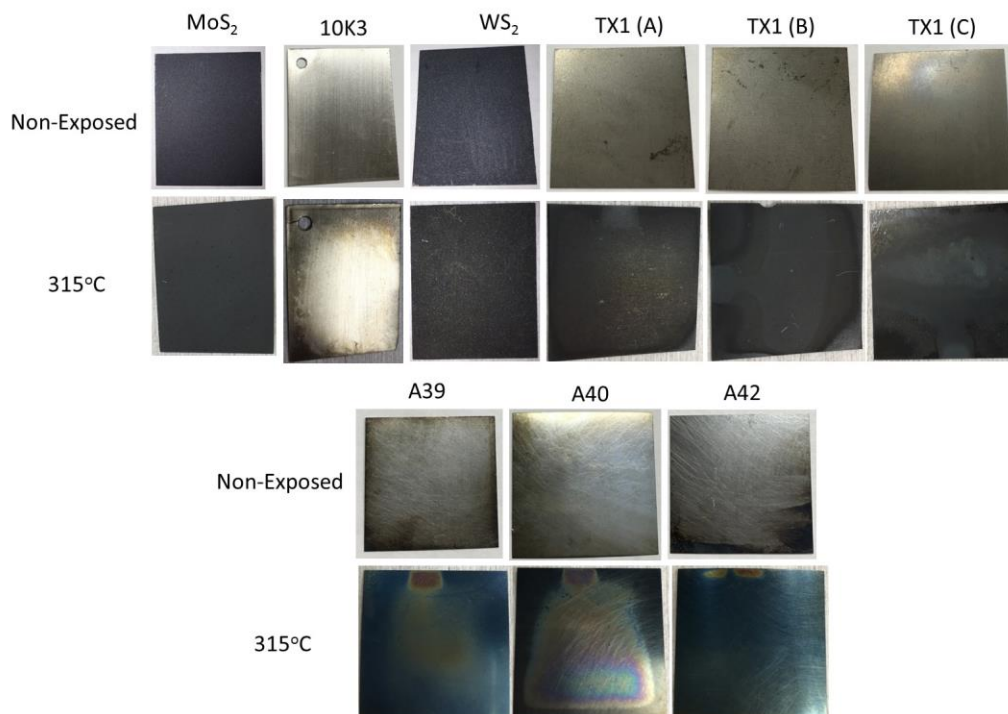


Figure 19. Visual changes for flat foil samples before and after the 315°C exposure test

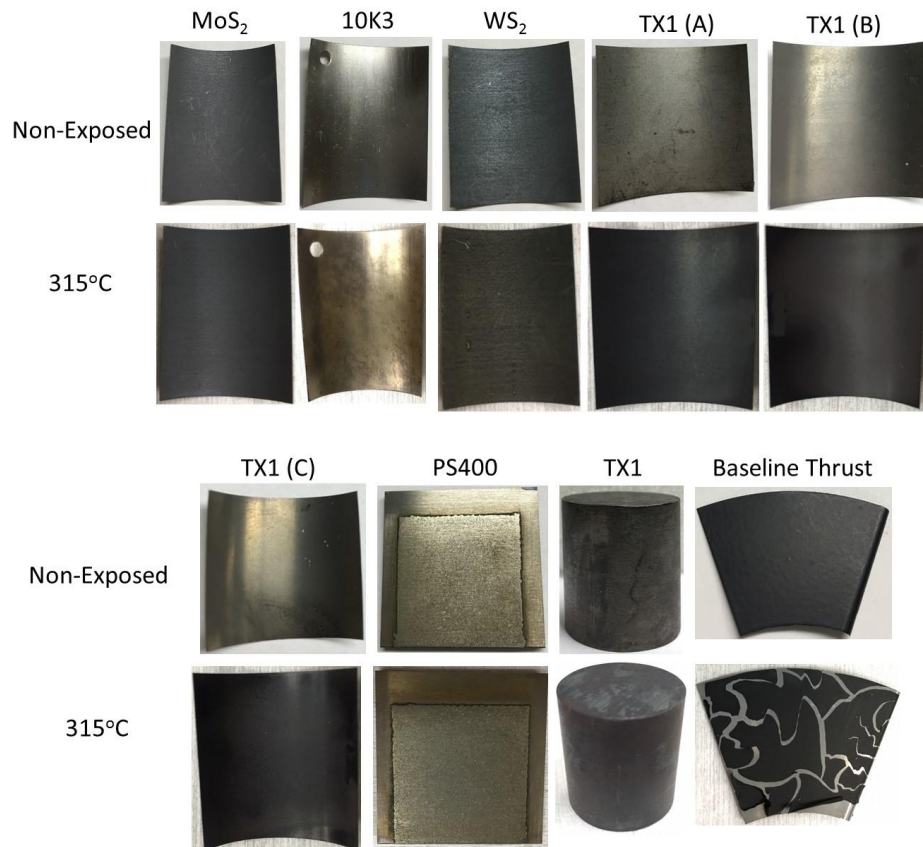


Figure 20. Visual changes for non-flat foil samples before and after the 315°C exposure test

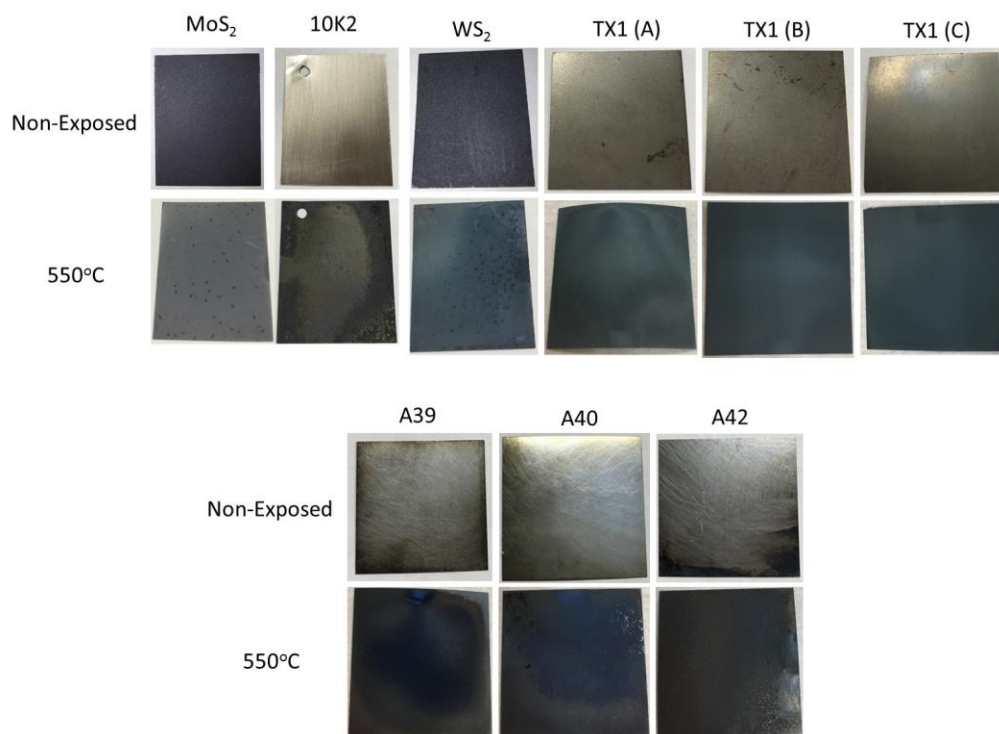


Figure 21. Visual changes for flat foil samples before and after the 550°C exposure test

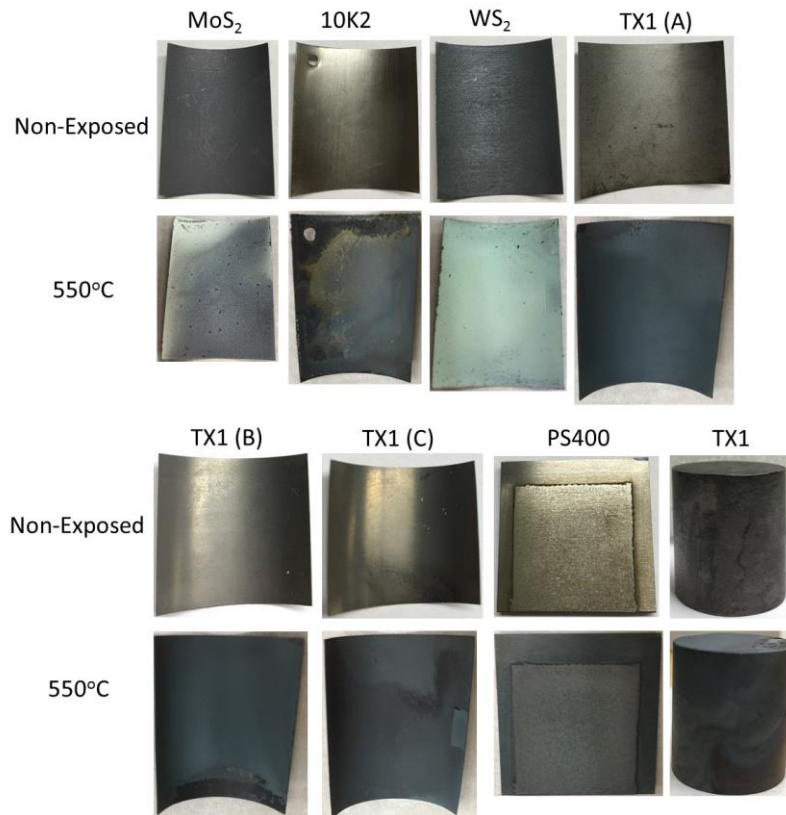


Figure 22. Visual changes for non-flat foil samples before and after the 550°C exposure test

4.2. Weight Change

Changes in sample weight following the exposure experiments can provide insight into their interactions with the environment. The most desirable scenario would be modest changes in sample weight. Weight change data are shown in Figure 23 for both of the exposure tests. Here, for the various types of coating, data are broken out by sample format (curved versus flat) in order to evaluate its influence on sample weight change. Data is reported as percentage weight gain versus the initial sample weight prior to exposure.

For the MoS_2 and WS_2 samples, weight loss was observed, and this appears to increase in moving to the higher exposure temperature. Other than these samples, all of the others exhibited weight gains at the higher temperature. This is believed to be associated to oxidation that has occurred at the interface of the alloy substrate to the coating; this is confirmed by microstructural analyses of samples. Worth noting, is that the samples with the largest weight gains were the 10K2 and TX1 samples.

For the case of the lower temperature exposure, many samples exhibited weight loss, and only the TX1 samples had gained weight. Samples with the most significant weight loss were the Mechanical Solutions samples (A39, A40, A42) along with the baseline thrust bearing foil. It is not clear why sample weight loss was much more common at the lower exposure temperature.

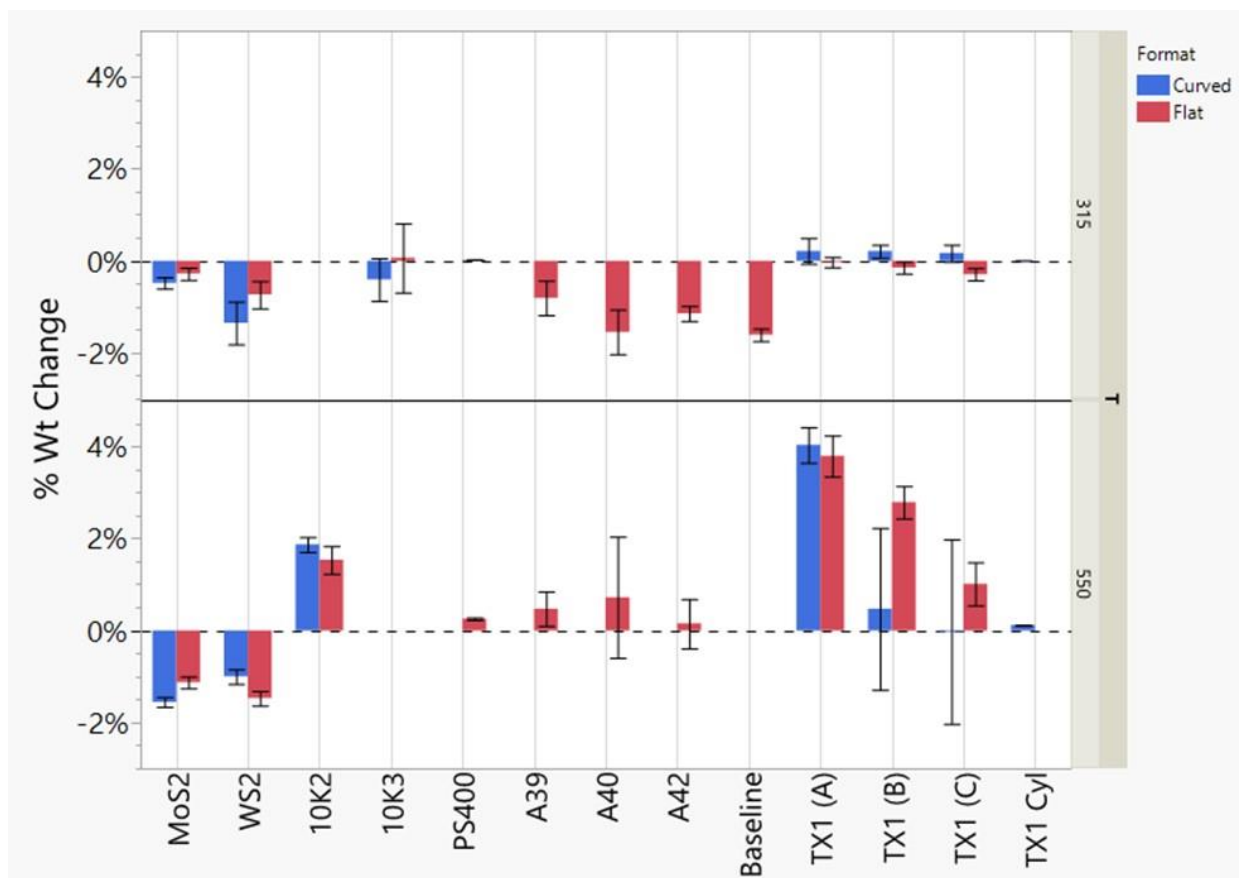


Figure 23. Sample weight changes following the exposure tests at 315°C and 550°C

4.3. Coating/Substrate Microstructure

While changes to sample weights can provide some information about what is happening to the coating during environmental exposure, a more complete picture of this interaction is provided when paired together with microstructural evaluation. SEM cross-sections of each of the sample types are compared for the three relevant conditions: Non-exposed, 315°C exposure, and 550°C exposure. These are shown for each of the samples in the flat format in Figure 24 and Figure 25. The plan was to also to examine cross-section microstructures for the curved foil samples, but these were not completed due to time constraints. All of these samples are available for future analysis if needed.

The most notable general observation for all of these samples, is that the lower temperature exposure resulted in relatively minor microstructural changes, while the higher temperature resulted in rather dramatic changes for many of the materials. An exception to this was the baseline thrust bearing foil sample which was observed to be severely degraded by the lower temperature exposure. Another exception was for both the MoS₂ and WS₂ samples, which didn't exhibit significant microstructural change at either exposure temperature.

Some samples exhibited extensive microstructural damage, which may preclude them from future consideration/testing as a bearing foil coating material. For the 315°C environment, the analysis suggests that the TX1 samples be eliminated from consideration. Chemical analysis of the corrosion products on the TX1 material is shown in Figure 26. While the nitrogen is still found near the surface and may be able to impart the desired hardness and wear resistance, an iron-based oxide is found on the surface that could spall and contribute to particulate generation within the bearing. The baseline thrust bearing coating also exhibited severe microstructural damage at the lower temperature. This may be attributable to a testing temperature above that which the bearing actually sees, since the degradation observed in this test was much more severe than is typically observed for these bearings. Nonetheless, it is good to know that other bearing coating materials are available that can tolerate this 315°C exposure temperature without the same degradation.

For the 550°C environment, several of the samples could be eliminated from consideration based on the severity of the microstructural damage observed. The TX1 sample oxidation, that was a problem at the lower temperature, was even more problematic at this higher temperature. Chemical analysis of the corrosion products on this sample are shown in Figure 27. The oxide is now much thicker and consists of an inner chrome-oxide layer and outer iron-oxide layer. This material should be eliminated from consideration in bearing foils at both of the exposure conditions. Also, the 10K2 coating is not recommended for use at this temperature due to coating delamination from the foil substrate. Chemical analysis of this coating is shown in Figure 28. The substrate surface was observed to be depleted in chromium, as a precipitated Cr-S phase was found within the Ni-P coating layer. This may have contributed to the coating delamination that was observed. Also, islands of a Ni-S phase were found on top of the coating surface, which may contribute to increased surface roughness.

Microstructural degradation was observed for both the PS400 as well as the Mechanical Solutions samples (A39, A40, A42) at the higher temperature, but neither should be precluded from future consideration based on this. In the case of the PS400, the coating material itself did not change. Instead, oxidation was observed to occur at the coating-substrate interface. A chemical analysis of the coating-substrate interface is provided in Figure 29, which shows the formation of iron-oxide at the interface. This is partially attributable to the substrate material, rather than to the coating. The PS400 was applied to a 15-5 stainless steel substrate, which is significantly more susceptible to corrosion in CO₂ environments than for the Inconel X750 substrates used with many of the other coatings. One could argue that the MoS₂ or WS₂ samples, which also did not exhibit obvious degradation of the coating material, would have demonstrated similar substrate oxidation as the PS400 if they had been put down on the 15-5 alloy rather than X750.

In the case of the three Mechanical Solutions coatings, they all appear to change following the high temperature exposure. It appears that the coating material either reacts with the substrate alloy or there is internal oxidation that occurs below the surface of the substrate. The coating material itself appears to remain intact and may indeed function well as a bearing coating. Due to the NDA that is established with them, the authors are unable to provide any additional information regarding the chemistry of the coating itself or any of the reaction products.

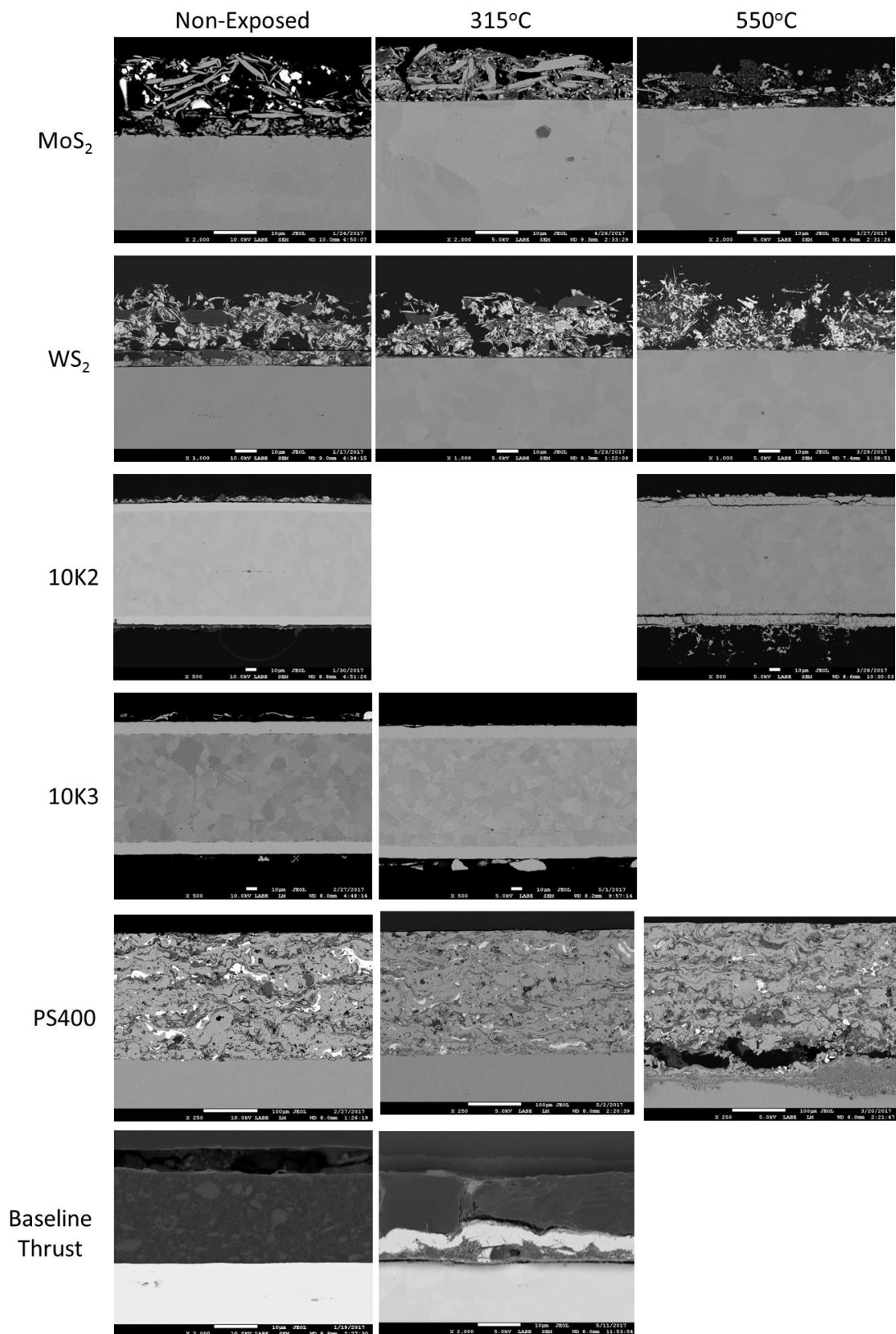


Figure 24. SEM cross-sections for one set of samples compared for the three conditions

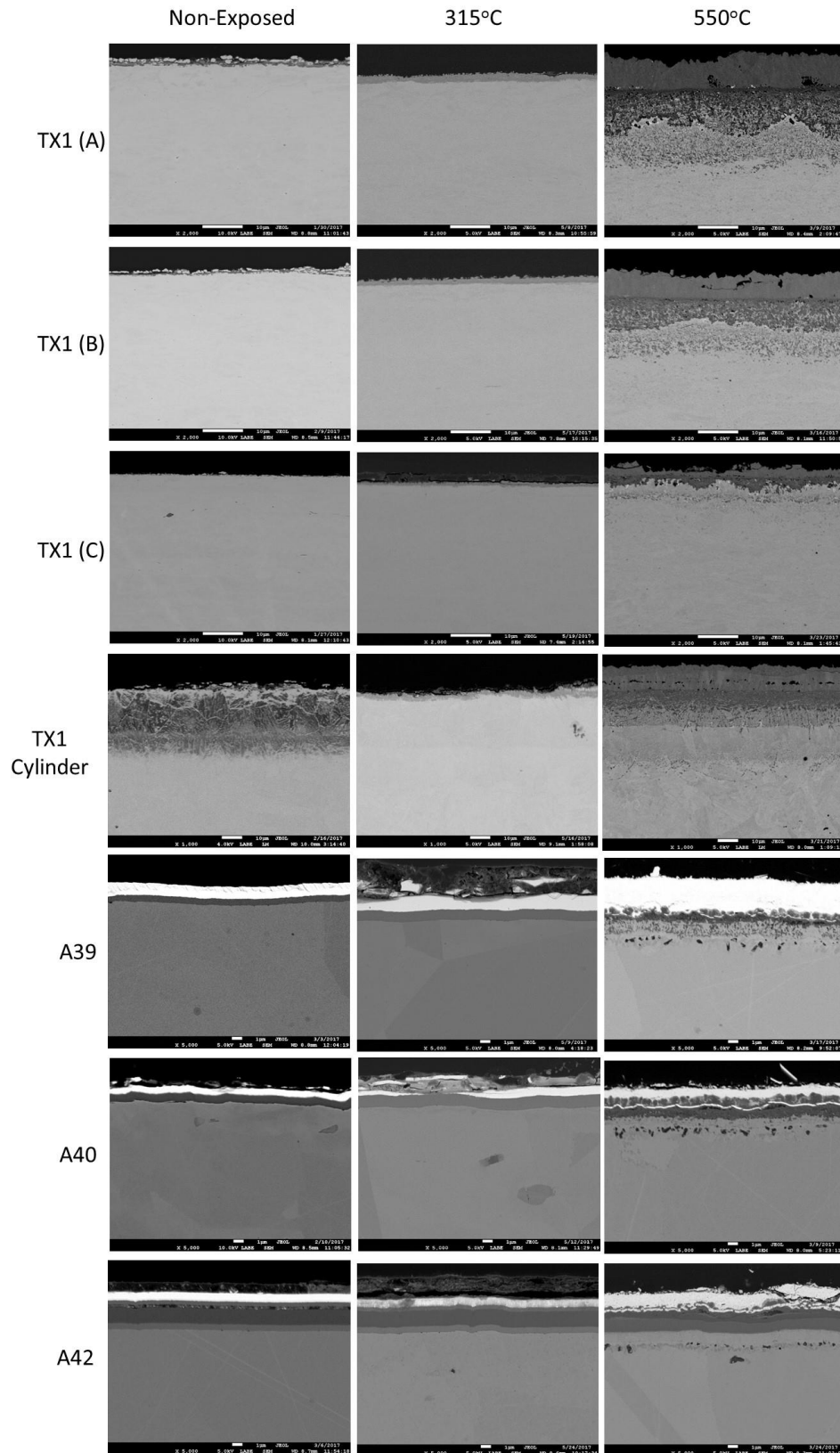


Figure 25. SEM cross-sections for a second set of samples compared for the three conditions

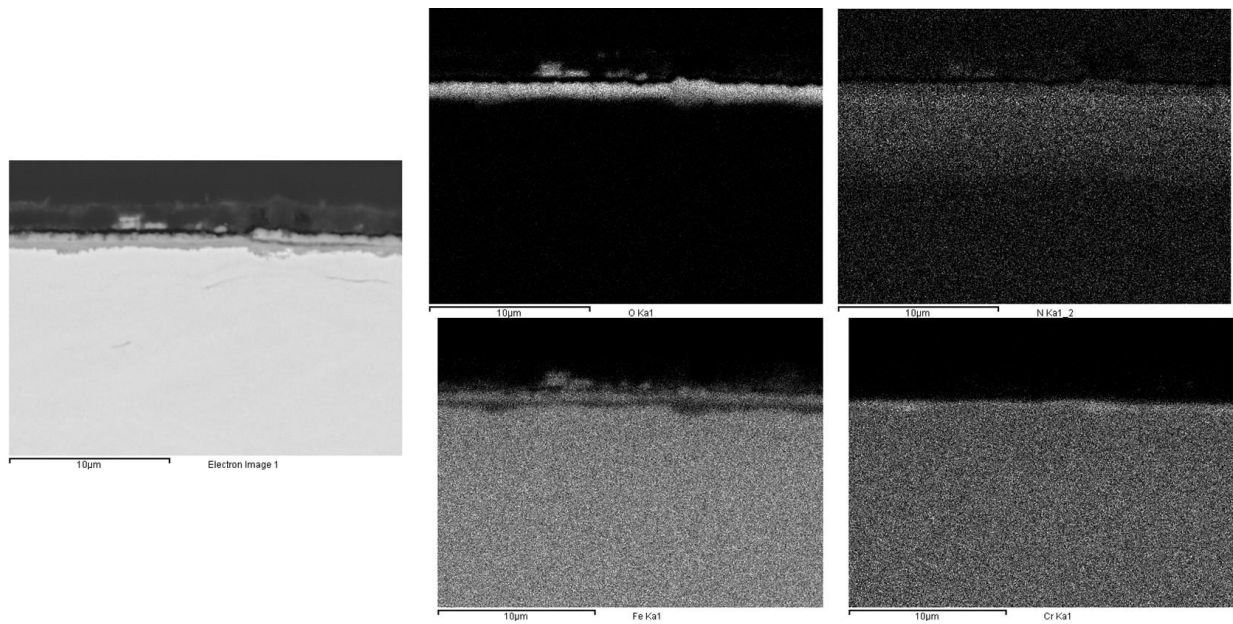


Figure 26. EDS chemical analysis for the TX1 coating exposed at 315°C

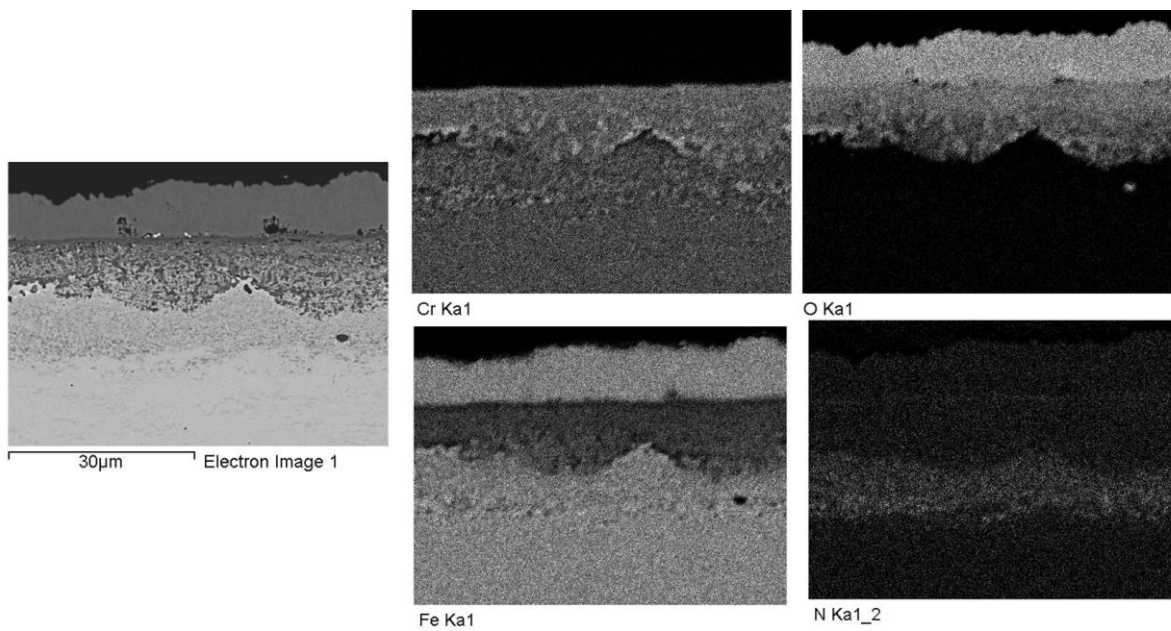


Figure 27. EDS chemical analysis for the TX1 coating exposed at 550°C

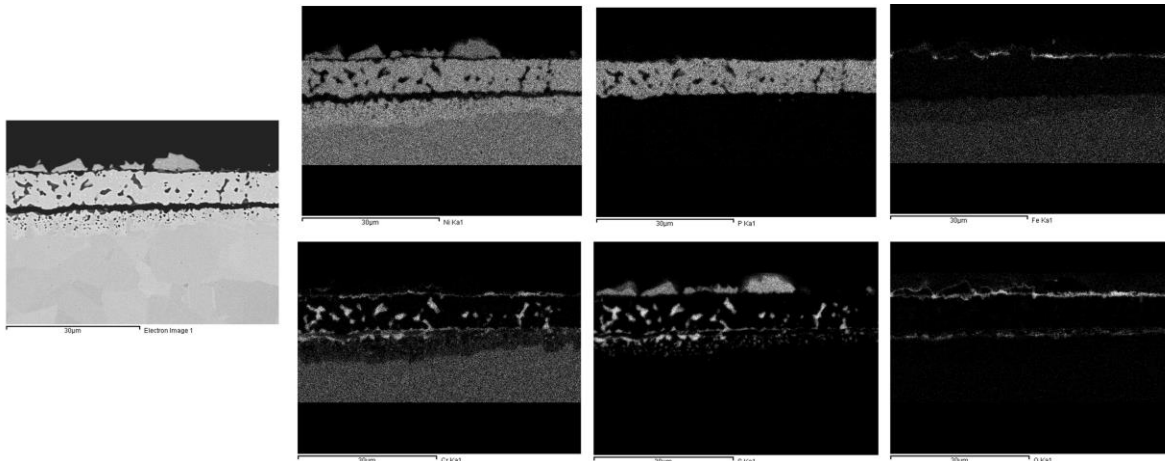


Figure 28. EDS chemical analysis for the 10K2 coating exposed at 550°C

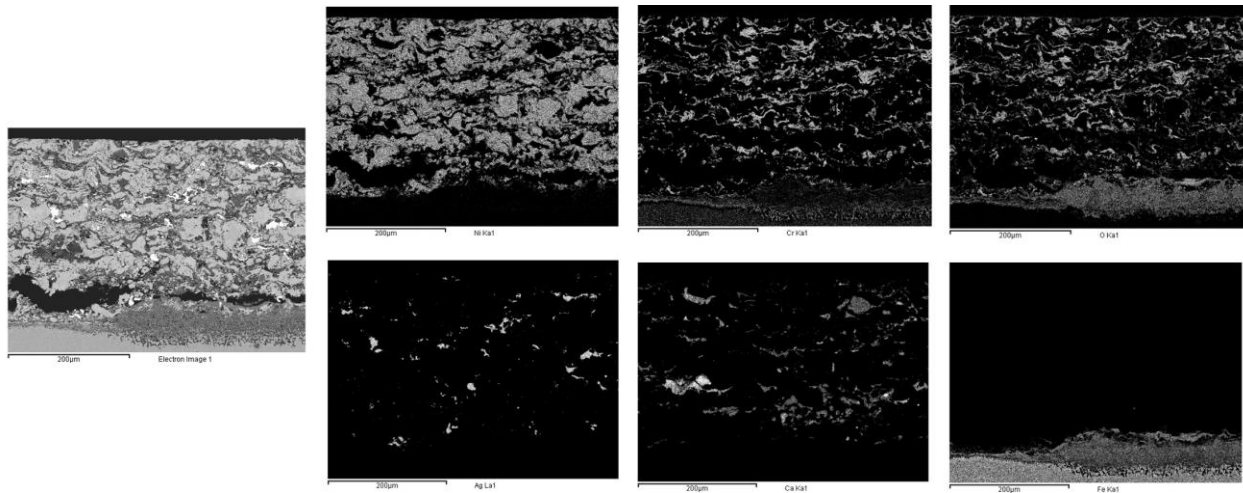


Figure 29. EDS chemical analysis for the PS400 coating exposed at 550°C

4.4. Surface Roughness

The surface roughness for samples are evaluated as a means of assessing how the various coating materials may be expected to perform in a bearing during rubbing. While it is only one variable of many that may contribute to its performance, a lower surface roughness is expected to improve bearing performance. It is useful to compare samples amongst themselves, but also to evaluate how sample roughness changes as a result of exposure to the high temperature, high pressure CO₂ environments.

Surface roughness values for the samples in the 315°C experiment are shown in Figure 30. The samples with the highest roughness are those with the MoS₂ and WS₂ coatings. The other coating

materials are comparable to each other, without significant differences. In general, the changes in surface roughness with the exposure environment were small, and generally decreased. An exception to this is the PS400 material which exhibited a large drop in surface roughness after exposure. In fact, it exhibited the lowest post-exposure surface roughness for any of the samples.

Visual observation of differences in sample surface roughness are illustrated in Figure 31. Here, 2D and 3D representations of a sample with low surface roughness, TX1 (A), are compared to those for a sample with much higher surface roughness, WS₂. The WS₂ materials is found to have peaks or islands on its surface, that contribute to its higher measured surface roughness. This is pointed out to establish a visual reference for what surface roughness differences look like for several of the coating materials.

Surface roughness values for the samples in the 550°C experiment are shown in Figure 32. Again, the MoS₂ and WS₂ samples are identified as having the highest surface roughness. Also, both materials are observed to have increasing surface roughness following the environmental exposure. In fact, most of the candidate materials exhibited increased surface roughness following the exposure, and the surface roughness values are higher than those from the lower temperature exposure. It is unclear what contributes to these trends, but future bearing-rig tests should be valuable to explore this in more depth.

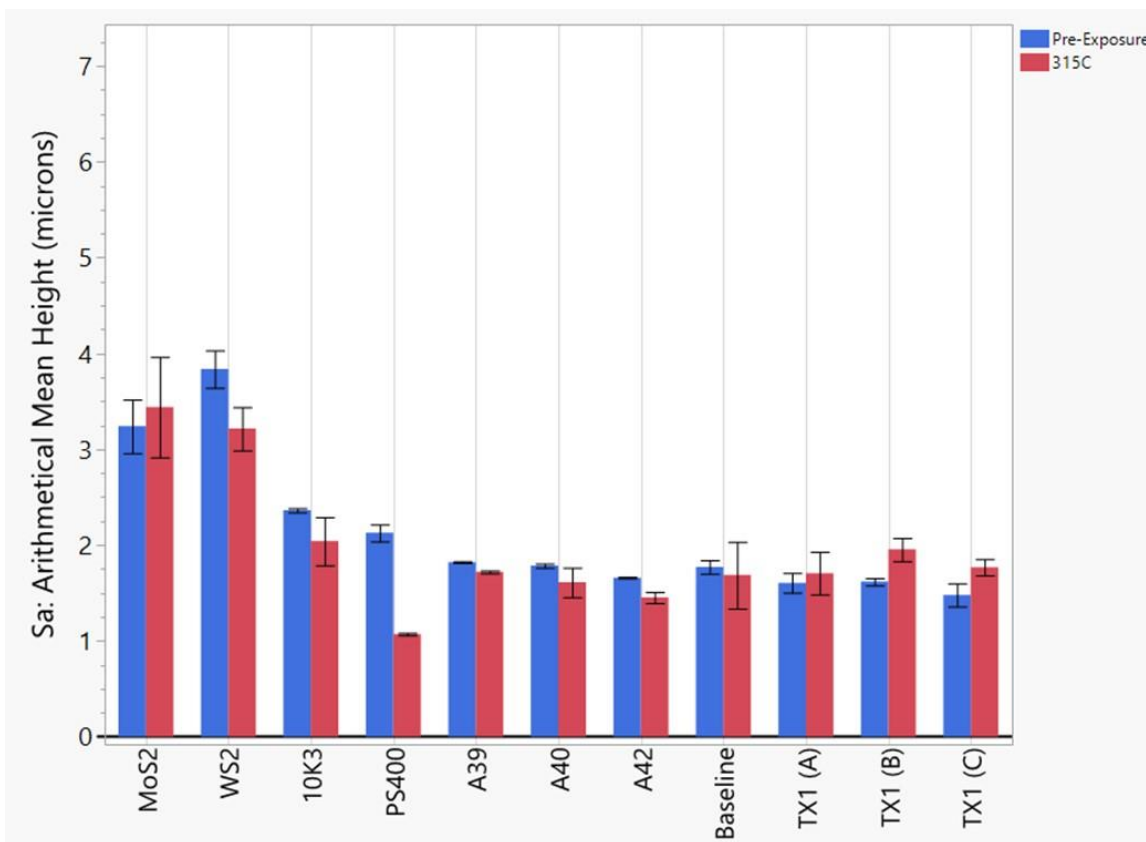


Figure 30. Surface roughness measurements for the 315°C exposure test samples

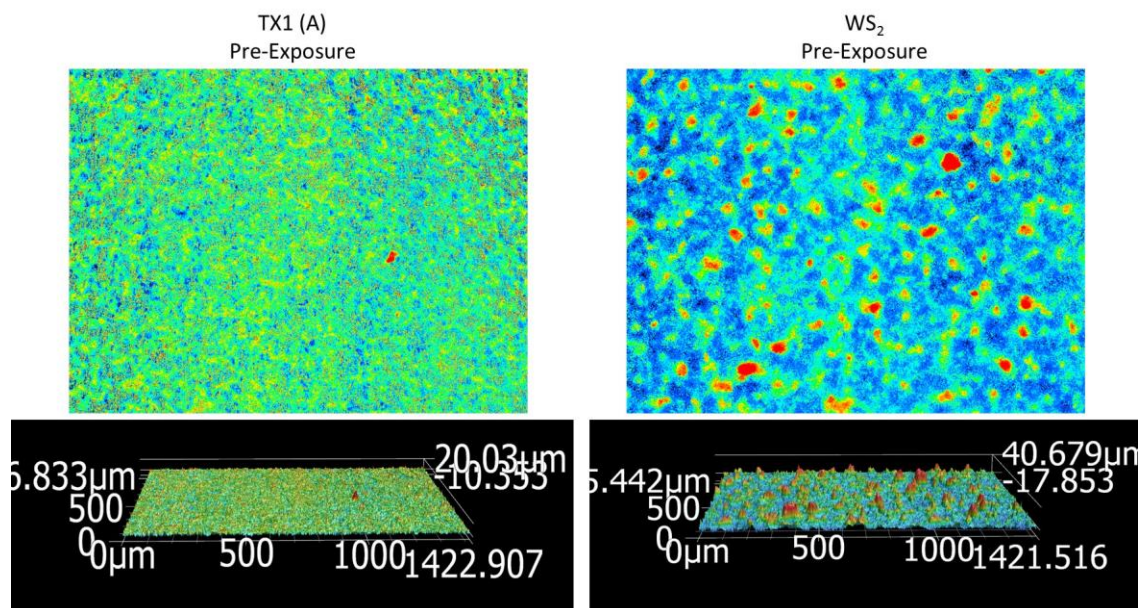


Figure 31. 2D and 3D representations for surface roughness for the TX1 and WS₂ coatings

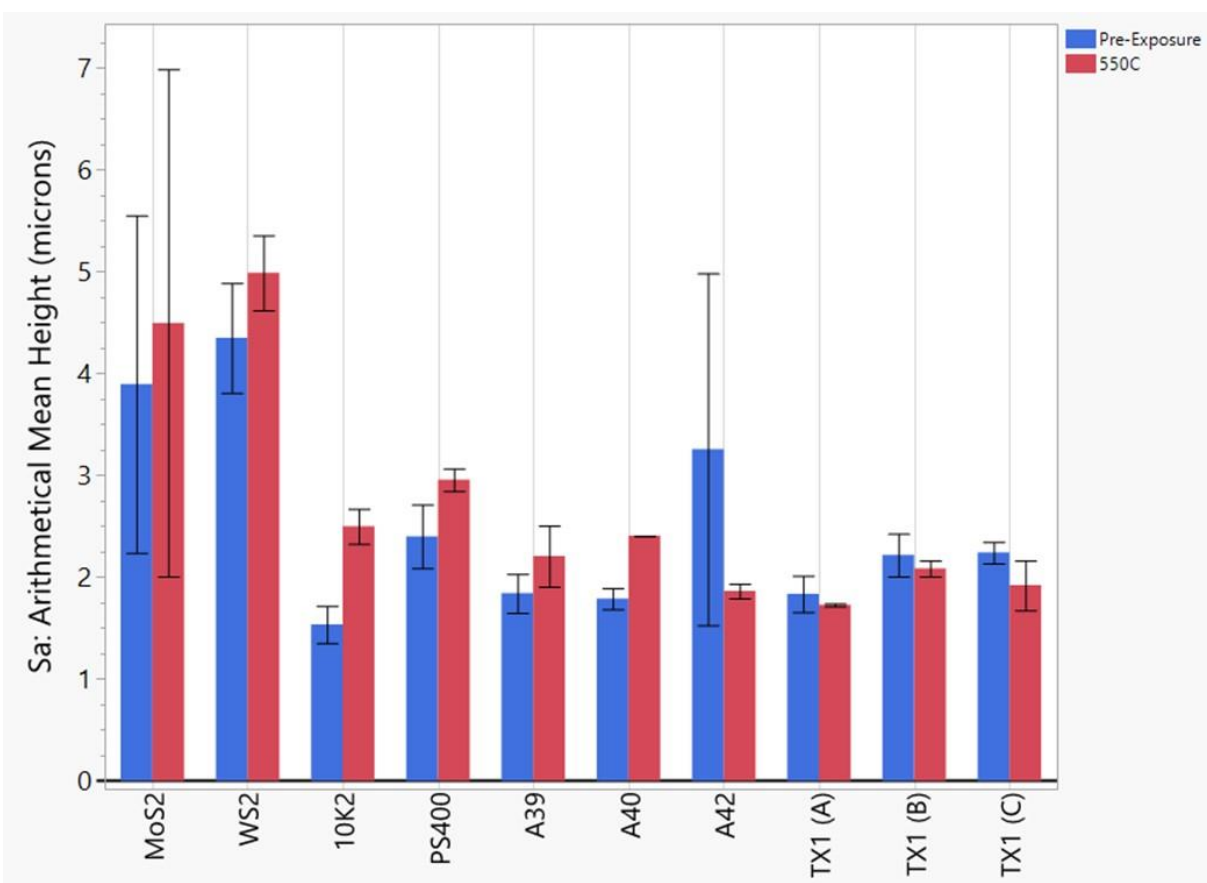


Figure 32. Surface roughness measurements for the 550°C exposure test samples

4.5. Scratch Testing

The two pieces of information obtained from the instrumented scratch testing are (1) the force at which coating cohesive failure occurs, and (2) the force at which coating adhesive failure occurs. The first relates to the ease with which the coating is able to be scratched or damaged, while the second relates to how strongly adhered the coating is to the substrate. Both are valuable metrics to consider in selecting bearing foil coating materials. High force values for both types of failure are desirable over low values.

The measured values for cohesive failure are provided for all of the coating materials at each of the test conditions (Pre-exposure, 315°C, and 550°C) in Figure 33. The WS₂ and Baseline thrust bearing coatings were the easiest to damage, and neither changed much with the environmental exposures. A legitimate concern for these samples would be the easy removal of the coating material from the bearing during rubbing. Some samples exhibited high damage resistance prior to exposure, but significantly lower resistance after exposures. This is particularly true for the MoS₂ and the three Mechanical Solution coatings (A39, A40, A42). For these samples, the changes in damage resistance were modest at the 315°C exposure, but decreased significantly at the 550°C exposure. For other samples, the damage resistance was low initially, but showed significant increase after environmental exposure. Obviously, this is preferable to the opposite scenario. This was observed for the 10K2, 10K3, and PS400 samples.

Measured values for adhesive failure are provided for the same coating materials at the same three test conditions in Figure 34. Similarly, to the cohesive failure values, two divergent trends are observed. For some of the samples, the coating adhesion was largest pre-exposure, and decreased with the environmental exposures. This was observed for the three Mechanical Solutions samples (A39, A40, A42), the Baseline thrust bearing coating, and the TX1 samples. Most dramatic among these were the Mechanical Solutions and Baseline samples. These started out with the best coating adhesion strengths, but dropped to some of the lowest values of any following the exposures. For the Mechanical Solutions coatings, the adhesion strengths were higher than any of the other materials following the 315°C exposure, but were some of the lowest values following the 550°C exposure. Samples exhibiting the opposite trend of increasing coating adhesion strength with environmental exposure, were the MoS₂, WS₂, 10K2, 10K3, and PS400 samples.

To summarize, the samples with the highest pre-exposure damage resistance were the Mechanical Solutions samples. These same samples also had the highest damage resistance after the 315°C exposure, while the sample with the highest damage resistance after the 550°C exposure were the PS400 sample. The samples with the highest pre-exposure adhesion strength were the Mechanical Solutions samples and the Baseline thrust bearing sample. Those with highest strength after the 315°C exposure were the Mechanical Solutions samples, and after the 550°C exposure were the MoS₂, WS₂, and PS400 samples.

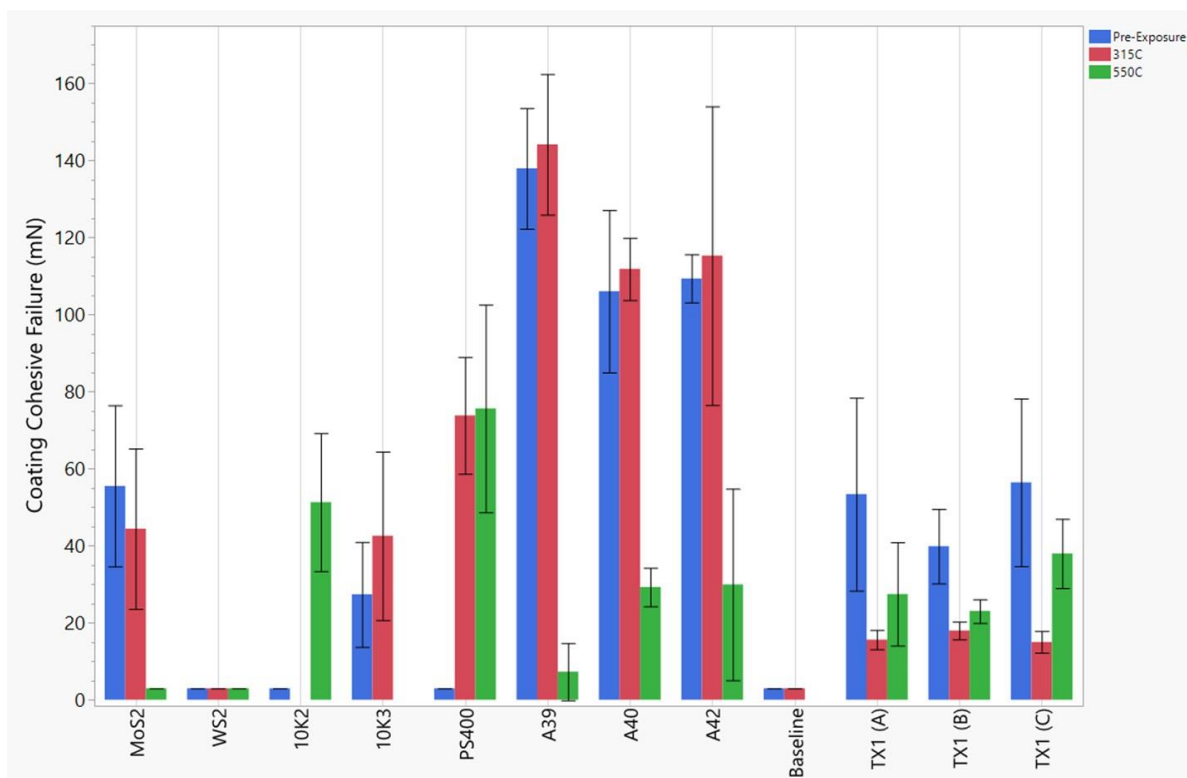


Figure 33. Measured cohesive failure values for each coating material at all exposure conditions

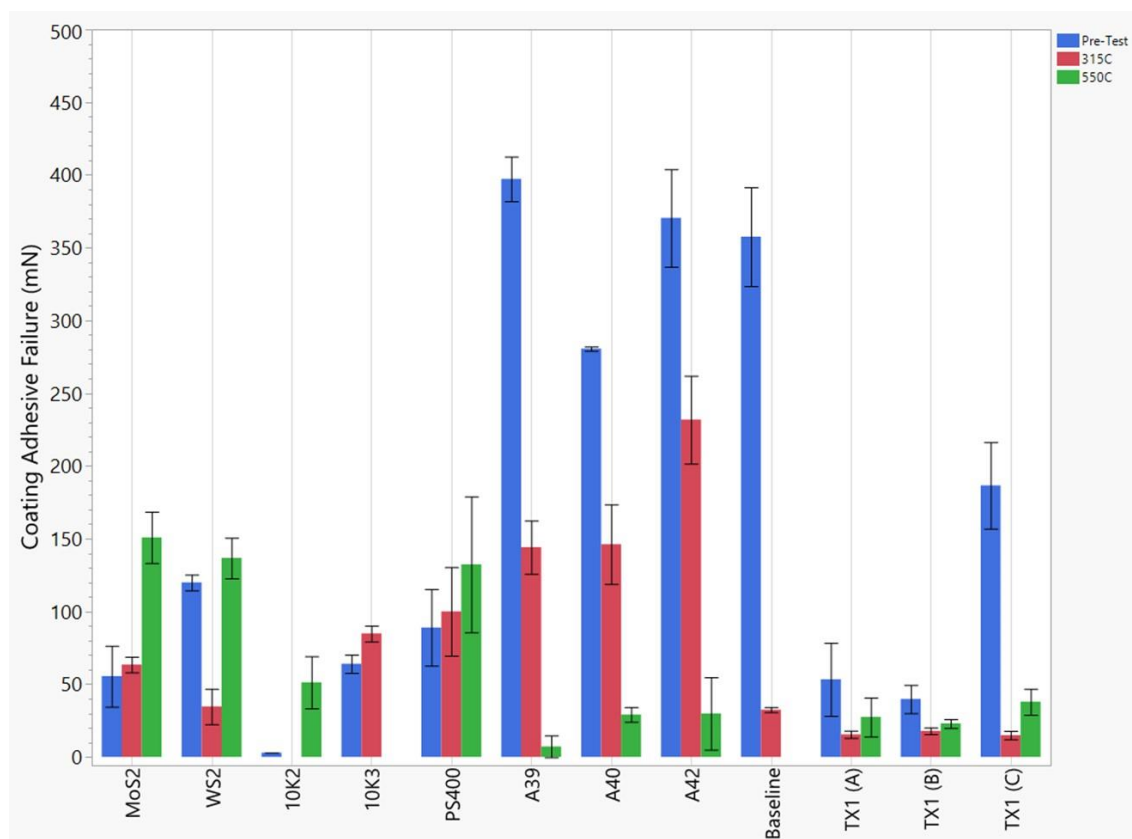


Figure 34. Measured adhesive failure values for each coating material at all exposure conditions

5. Summary

A need was identified for evaluating gas foil bearing coating materials in environments relevant to S-CO₂ power systems. In response to this need, a test configuration was developed enabling long duration exposure tests, followed by a range of analyses relevant to their performance in a bearing. Analysis by members of the Sandia S-CO₂ team in Albuquerque, NM established a pressure of 300 psi CO₂ at both the turbine-side and compressor-side bearings. Additionally, a temperature of 550°C was established for the turbine-side bearings, and a temperature of 315°C was established for the compressor-side. Long duration (500 hours) experiments at both conditions, provide valuable data regarding the performance of bearing coating materials in these environments. This report provides a detailed overview of this work, which involved significant collaboration with industrial gas foil bearing vendors. The results contained herein provide valuable information in selecting appropriate coatings for more advanced future bearing-rig tests at the newly established test facility in Sandia-NM.

Sample performance was assessed across several different areas following environmental exposures. These included visual observations, weight change, coating/substrate microstructure, surface roughness, and scratch testing. Based on these analyses, a series of recommendations are made for materials to include in future bearing-rig tests at Sandia in Albuquerque, NM.

The TX1 coating materials performed poorly in many of the categories and should be eliminated from future consideration. The most prominent problem with these are their associated surface oxidation, which would lead to particulate generation within the bearing. The baseline thrust bearing coating (Teflon-based) also performed poorly across several categories. It is easily damaged both before and after environmental exposure, and the coating adhesion strength is significantly reduced following the 315°C exposure. Significant cracking/peeling of the coating along the foil surface was also observed. These are not observed for this material following operation in the Sandia RCBC, and so it is possible that 315°C is a higher temperature than the thrust bearing truly experiences. Conversely, it is possible that it does see this temperature in the RCBC, but that the short duration exposures don't reveal the degradation that this long duration exposure has revealed. A third material that should be eliminated from consideration is the 10K2 Nickel based coating. This material, being considered for only the higher temperature environment, exhibited significant delamination from the substrate following the exposure test.

Each of the other coating materials (10K3, MoS₂, WS₂, PS400, and the three Mechanical Solutions materials) are recommended for additional performance evaluations as bearing coating materials. The 10K3 material, being considered for only the 315°C condition, performed well in all areas of testing. The MoS₂ and WS₂ coatings, appeared to be very stable in the exposure environments, and together with the PS400 material, had the highest coating adhesion strength after the 550°C exposure. On the negative side, they had the highest surface roughness and very low damage resistance following the 550°C exposure. The PS400 material was very stable in the environments, had the best post-exposure damage resistance in both environments, and had very high coating adhesion strength following both exposures. It also exhibited the lowest surface roughness after the 315°C exposure. As a negative, substrate oxidation was observed for the

550°C exposure, but the change to the 15-5 stainless steel alloy here in place of the Inconel X750 substrate used for the foil samples, certainly played a role. Finally, the three Mechanical Solutions materials exhibited good surface roughness, had the highest damage resistance and substrate adhesion strength as pre-exposed and 315°C exposed. For the 550°C exposure they didn't perform so well in these two areas. A reaction is believed to occur between the coating material and substrate at this higher temperature, and this may be contributing.

REFERENCES

1. McHugh, J.D. (1979). Principles of Turbomachinery Bearings. In: Proceedings of the 8th Turbomachinery Symposium, Texas A&M University, 135-144.
2. Brun, K., et al. (2017). *Fundamentals and Applications of Supercritical Carbon Dioxide (SCO₂) Based Power Cycles*. Woodhead Publishing.
3. Chapman, P.A. (2016). Advanced gas foil bearing design for supercritical CO₂ power cycles. In: The 5th International Symposium - Supercritical CO₂ Power Cycles, San Antonio, Texas.
4. Ahn, Y., et al. (2015). Review of Supercritical CO₂ Power Cycle Technology and Current Status of Research and Development, Nuclear Engineering Technology (47), 647-661.
5. Cho, J., et al. (2016). Research on the Development of a Small-Scale Supercritical Carbon Dioxide Power Cycle Experimental Test Loop. In: Proceedings of the 5th International Symposium – Supercritical CO₂ Power Cycles, March 28-31, San Antonio, Texas.
6. Preuss, J.L. (2016). Application of hydrostatic bearings in supercritical CO₂ turbomachinery. In: Proceedings of the 5th International Symposium – Supercritical CO₂ Power Cycles, March 28-31, San Antonio, Texas.
7. Devitt, D. (2016). Porous externally pressurized gas bearings. In: Proceedings of the 5th International Symposium - Supercritical CO₂ Power Cycles, March 29 - 31, San Antonio, Texas.
8. Conboy, T. (2012). Gas Bearings and Seals Development for Supercritical CO₂ Turbomachinery, Sandia Report: SAND2012-8895.
9. DellaCorte, C., Edmonds, B. (2009). NASA PS400: A New High Temperature Solid Lubricant Coating for High Temperature Wear Applications, NASA Report: 2009-215678.
10. DellaCorte, C., et al (2010). The Effect of Composition on the Surface Finish of PS400: A New High Temperature Solid Lubricant Coating, NASA Report: 2010-216774.
11. Walker, M., et al (2016). Progress in Overcoming Materials Challenges with S-CO₂ RCBCs: Final Report, Sandia Report: SAND2016-9774.